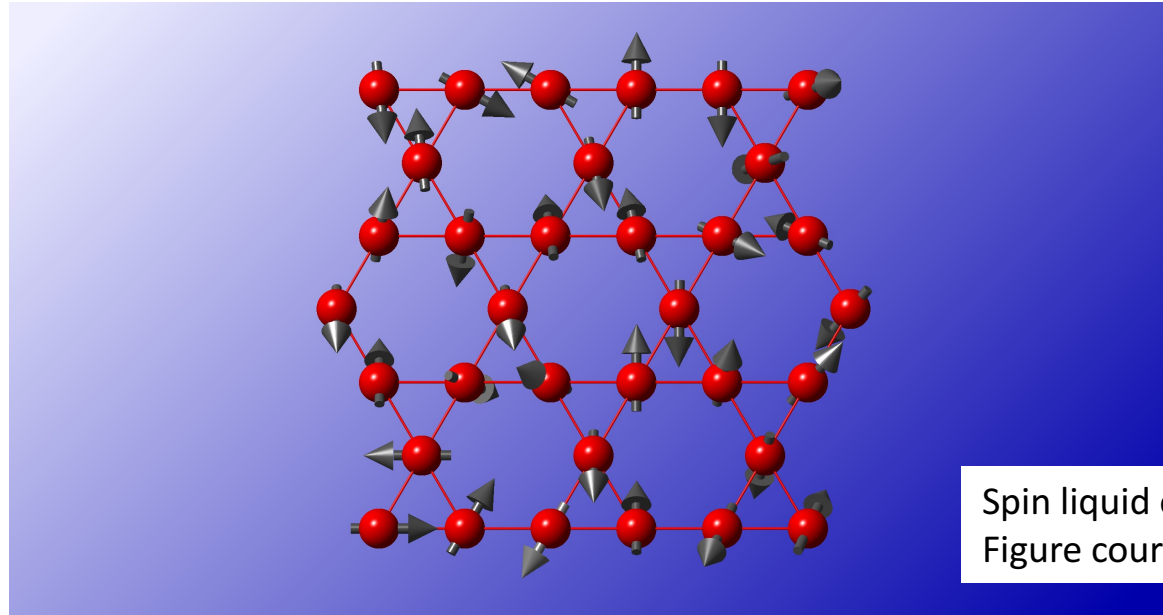


**NMR Evidence for a gapped spin-liquid ground state  
in a kagome Heisenberg antiferromagnet (herbertsmithite  $\text{ZnCu}_3(\text{OH})_6\text{Cl}_2$ )**

**Takashi Imai**

**McMaster University**

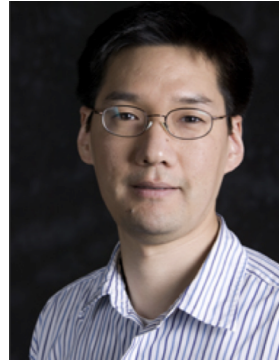
**Canadian Institute for Advanced Research**



## A Short List of Recent Collaborators



Dr. Mingxuan Fu  
McMaster  
→PDF at Johns Hopkins  
→NSERC PDF at Univ. of Toronto



Prof. Y.S. Lee  
M.I.T. → Stanford  
(Neutron / X'tal growth)



Dr. T. H. Han  
M.I.T. → Chicago/Argonne Nat. Lab.  
(Neutron / X'tal growth)



Prof. R.R.P. Singh  
U.C. Davis  
(Series expansion)



N.E. Sherman  
U.C. Davis  
(Series expansion)

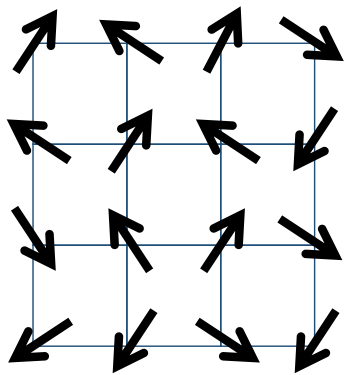
# Outline

1. Introduction: kagome lattice in herbertsmithite, and why NMR is useful  
T. Imai and Y.S. Lee., *Physics Today*, p-30, August (2016).
2. First generation  $^{35}\text{Cl}$ ,  $^1\text{H}$ , and  $^{63}\text{Cu}$  powder NMR measurements  
T. Imai *et al.*, *PRL* [100](#) (2008) 077203
3. Second generation single crystal  $^2\text{D}$  NMR measurements on  $\text{ZnCu}_3(\text{OD})_6\text{Cl}_2$   
T. Imai *et al.*, *PRB* [83](#)(2011) 020411 (Rapid).
4. Third generation single crystal  $^{17}\text{O}$  NMR measurements on  $\text{ZnCu}_3(\text{OH})_6\text{Cl}_2$   
M. Fu, T. I. *et al.*, *Science* [350](#) (2015) 655.  
N. Sherman, T.I., R.R.P. Singh, *PRB* 94 (2016) 140405. [Series expansion.]
5. Summary

# Paramagnetic ground state vs. antiferromagnetic phases

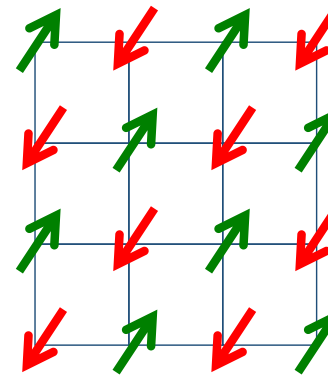
Antiferromagnetic “Heisenberg model” (model Hamiltonian)

$$\hat{H} = J \sum_{\langle i,j \rangle} \hat{S}_i \cdot \hat{S}_j \quad (J > 0)$$



Higher temperatures

Paramagnetic state with randomly oriented spins



$T \leq T_N$   
(Neel temperature)

Neel state : usually, spins are antiferromagnetically ordered with a regular pattern ( $T_N=0$  for square-lattice)

In analogy with.....



Liquid water

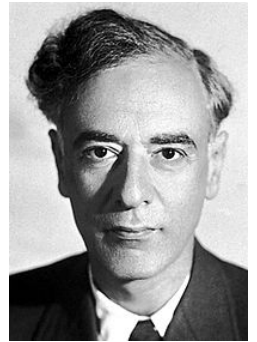


Solid ice  
 $T < 273 \text{ K}$

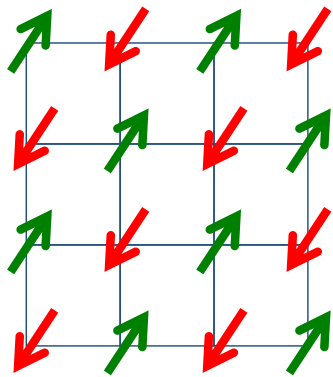
# Old controversy: Antiferromagnetically ordered state vs. Landau's superposed singlets

Antiferromagnetic "Heisenberg model"  
(model Hamiltonian)

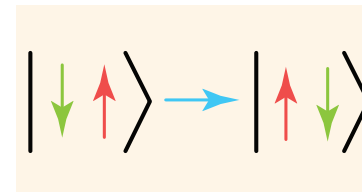
$$\hat{H} = J \sum_{\langle i,j \rangle} \hat{S}_i \cdot \hat{S}_j \quad (J > 0)$$



"Neel state" is not an eigenstate of the Hamiltonian.

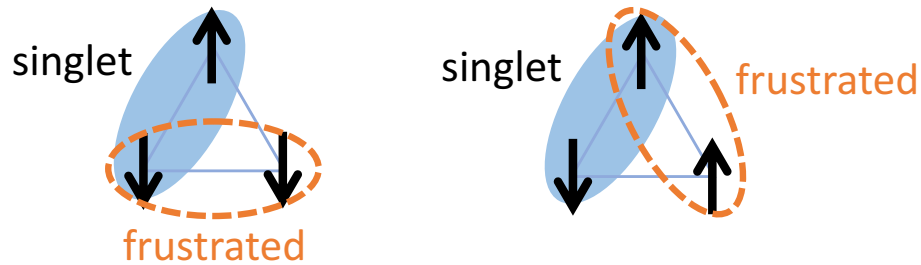


Landau (1962 Nobel Physics) thought *there is no such a thing as antiferromagnetically ordered state*; Instead, *superposed singlet states must be realized*.



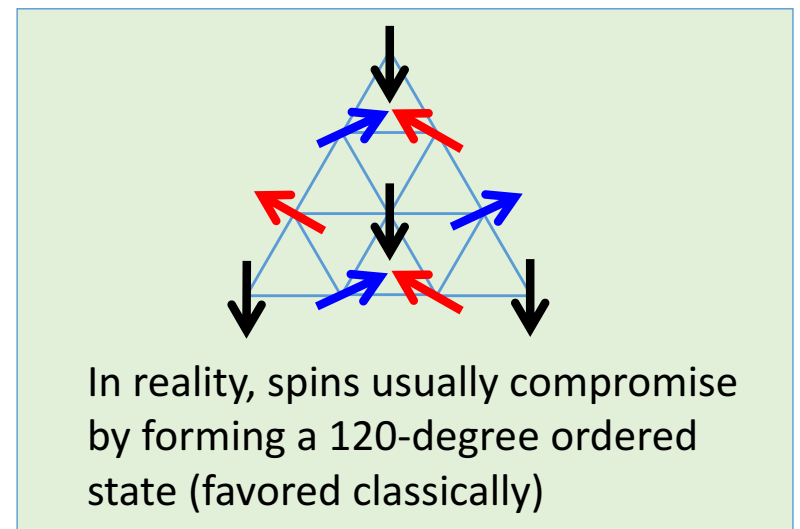
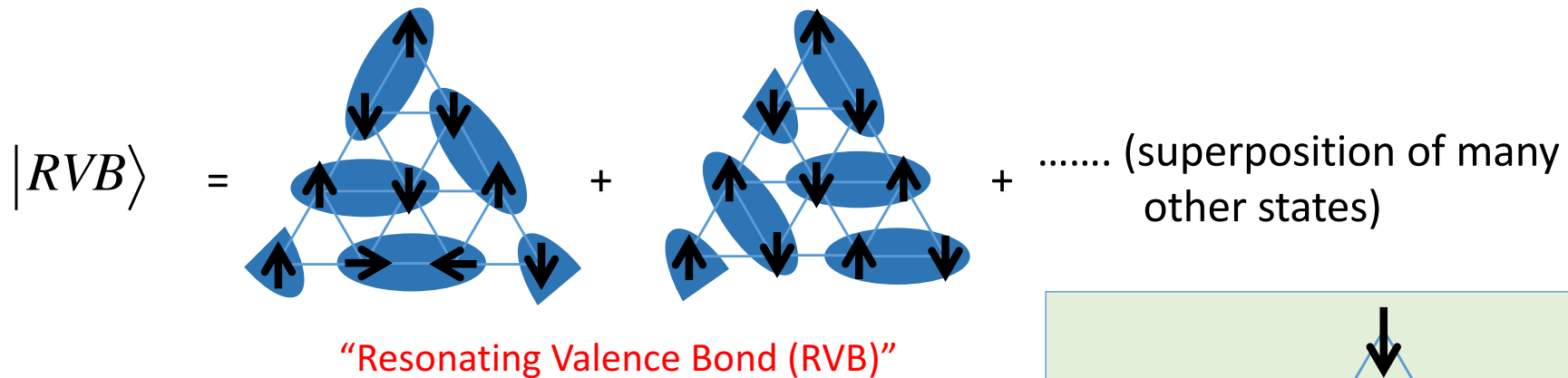
Mostly forgotten idea for decades, because antiferromagnets do exist after all.

# Geometrical frustration effects of spins on the triangular-lattice Heisenberg model and the **RVB** “spin liquid” (P.W. Anderson 1973)



Frustration effects arise from love-and-hate relationship between  $S=1/2$  spins on a triangle

P.W. Anderson (Nobel physics 1977)





Where should we look for a quantum spin liquid?

“Kagome” 籠目 : “Basket pattern” composed of **corner-sharing triangles**

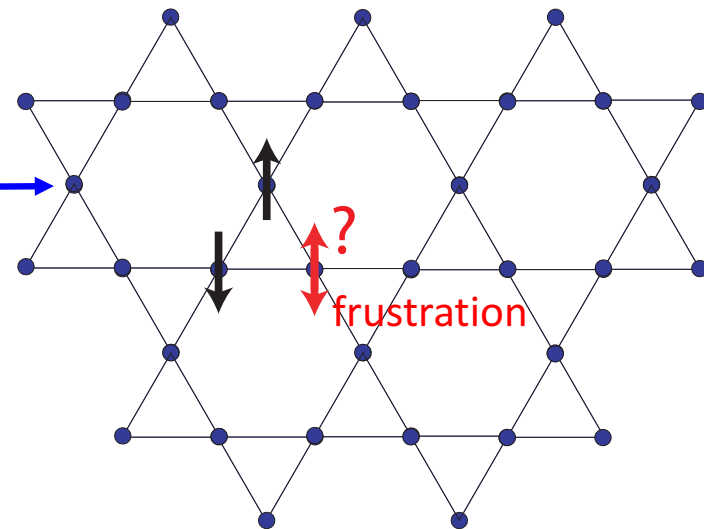


“Basket pattern”  
(kago) (me)  
籠 目



Japanese “Kagome Tomato Ketchup”

Corner-sharing triangles

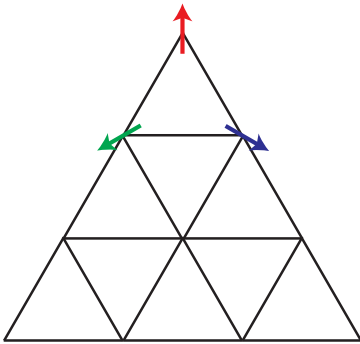


Advantage of the kagome Heisenberg antiferromagnet = (strong degeneracy).

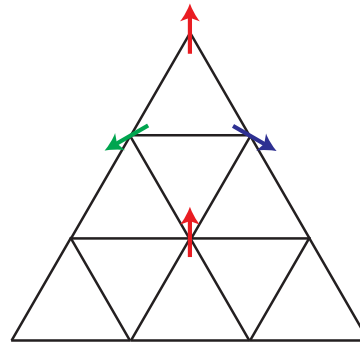
Favors a quantum spin liquid ground state

### Edge-sharing triangular lattice

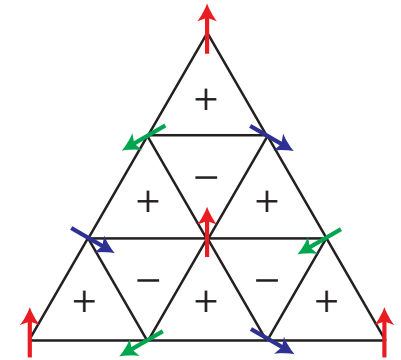
120 degree arrangement on a triangle minimizes the energy (classically)



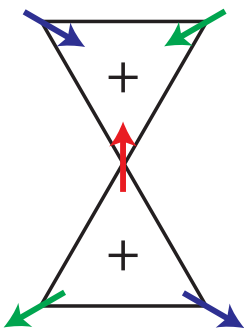
... and constrains another spin



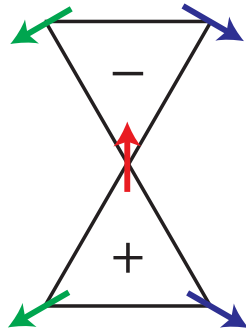
... and all spins



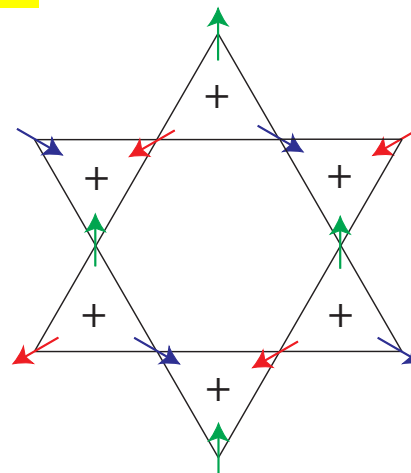
### Corner-sharing triangular lattice (kagome)



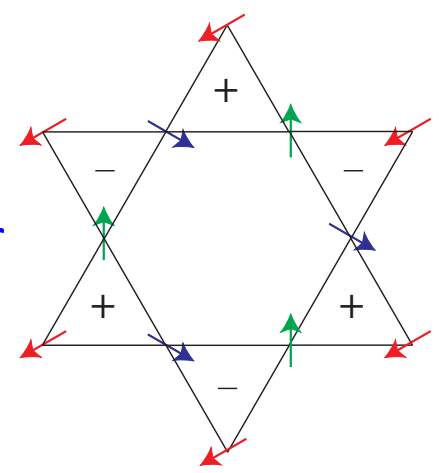
or



One triangle does not constrain the arrangement of the adjacent triangle



or



Spins have a hard time to choose ordering pattern!

# “The ground state of the kagome Heisenberg antiferromagnet is a gapped $Z_2$ spin liquid”

## Spin-Liquid Ground State of the $S = 1/2$ Kagome Heisenberg Antiferromagnet

Simeng Yan,<sup>1</sup> David A. Huse,<sup>2,3</sup> Steven R. White<sup>1\*</sup>

We use the density matrix renormalization group to perform accurate calculations of the ground state of the nearest-neighbor quantum spin  $S = 1/2$  Heisenberg antiferromagnet on the kagome lattice. We study this model on numerous long cylinders with circumferences up to 12 lattice spacings. Through a combination of very-low-energy and small finite-size effects, our results provide strong evidence that, for the infinite two-dimensional system, the ground state of this model is a fully gapped spin liquid.

We consider the quantum spin  $S = 1/2$  kagome Heisenberg antiferromagnet (KHA) with only nearest-neighbor isotropic exchange interactions (Hamiltonian  $H = \sum \vec{S}_i \cdot \vec{S}_j$ , where  $\vec{S}_i$  and  $\vec{S}_j$  are the spin operators for sites  $i$  and  $j$ , respectively) on a kagome lattice (Fig. 1A). This frustrated spin system has long been thought to be an ideal candidate for a simple, physically realistic model that shows a spin-liquid ground state ( $I-3$ ). A spin liquid is a magnetic system that has “melted” in its ground state because of quantum fluctuations, so it has

no spontaneously broken symmetries (4). A key problem in searching for spin liquids in two-dimensional (2D) models is that there are no exact or nearly exact analytical or computational methods to solve infinite 2D quantum lattice systems. For 1D systems, the density matrix renormalization group (DMRG) (5, 6), the method we use here, serves in this capacity. In addition to its interest as an important topic in quantum magnetism, the search for spin liquids thus serves as a test-bed for the development of accurate and widely applicable computational methods for 2D many-body quantum systems.

<sup>1</sup>Department of Physics and Astronomy, University of California, Irvine, CA 92617, USA. <sup>2</sup>Department of Physics, Princeton University, Princeton, NJ 08544, USA. <sup>3</sup>Institute for Advanced Study, Princeton, NJ 08540, USA.

\*To whom correspondence should be addressed. E-mail: srwhite@uci.edu

www.sciencemag.org SCIENCE VOL 332 3 JUNE 2011

1173

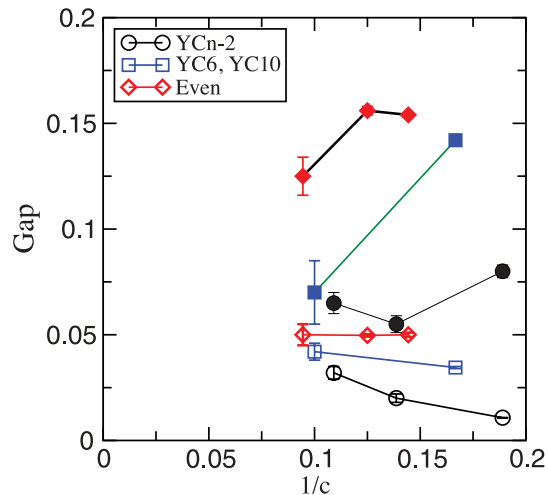


**Fig. 4.** Spin triplet (solid symbols) and singlet (hollow symbols) gaps for various cylinders with circumferences  $c$ . The type of cylinder ( $15$ ) is indicated in the key (inset).

Large scale DMRG (Density Matrix Renormalization Group) calculations

Yan, Huse, and White, *Science* **332** (2011) 1173.

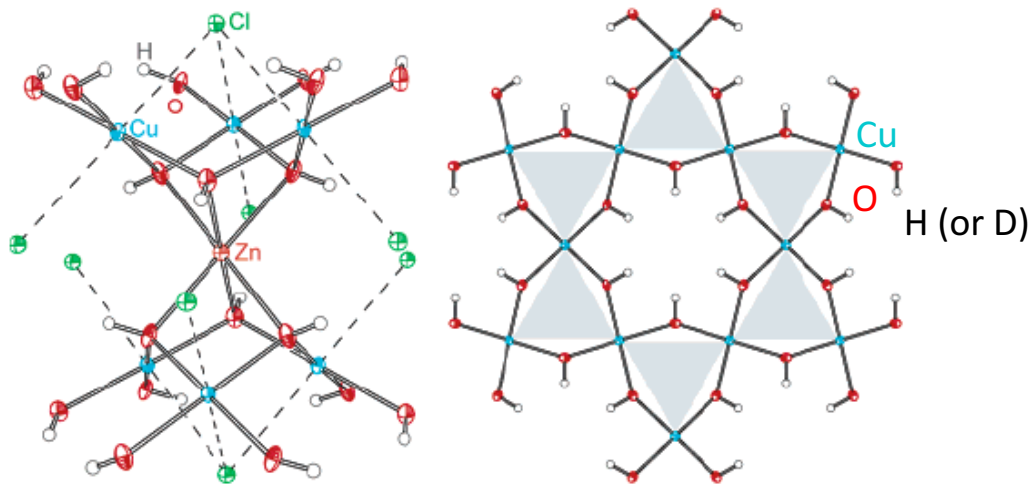
Also see Jiang *et al.*, *PRL* **101** (2008) 117203;

Deepenblock *et al.*, *PRL* **109** (2011) 067201;

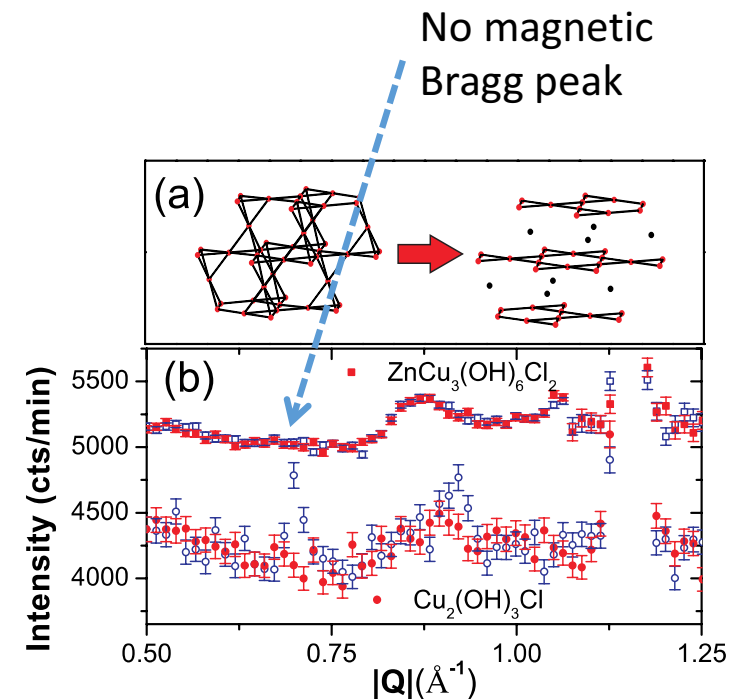
Liao *et al.*, *PRL* **118** (2017) 137202.

# Successful laboratory-synthesis of the structurally ideal kagome lattice Herbertsmithite $\text{ZnCu}_3(\text{OH})_6\text{Cl}_2$

M.P. Shores, D. Nocera *et al.* (M.I.T. Chemistry)  
J. Amer. Chem. Soc. **127**, (2005) 13462



- $\text{Cu}^{2+}$  ions ( $S = \frac{1}{2}$ ) form a perfect kagome lattice
- Cu-Cu super-exchange interaction  $J \sim 200$  K



Paramagnetic down to  $\sim 50$  mK

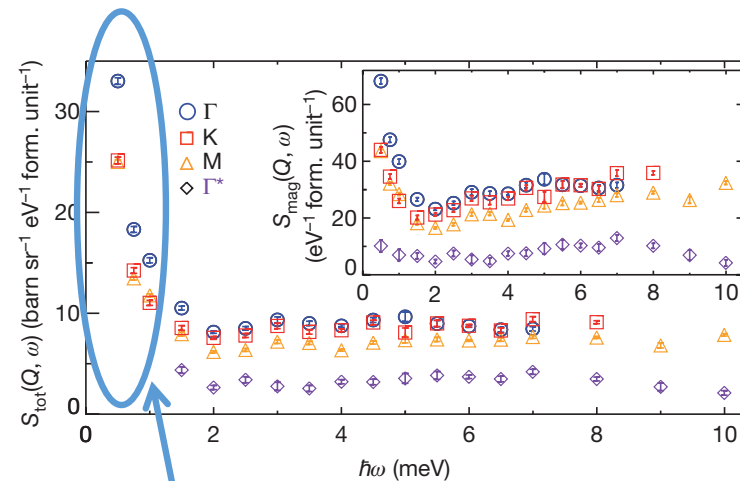
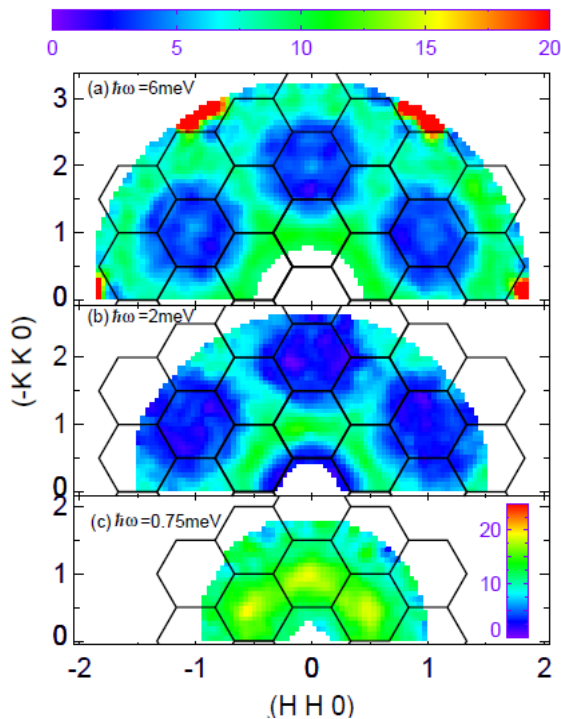
Helton *et al.* PRL 98 (2007) 107204.

Also by  $\mu\text{SR}$ , see Mendels *et al.*,  
PRL 98 (2007) 077204.

# Absence of conventional magnon excitations in $\text{ZnCu}_3(\text{OH})_6\text{Cl}_2$ in inelastic neutron scattering

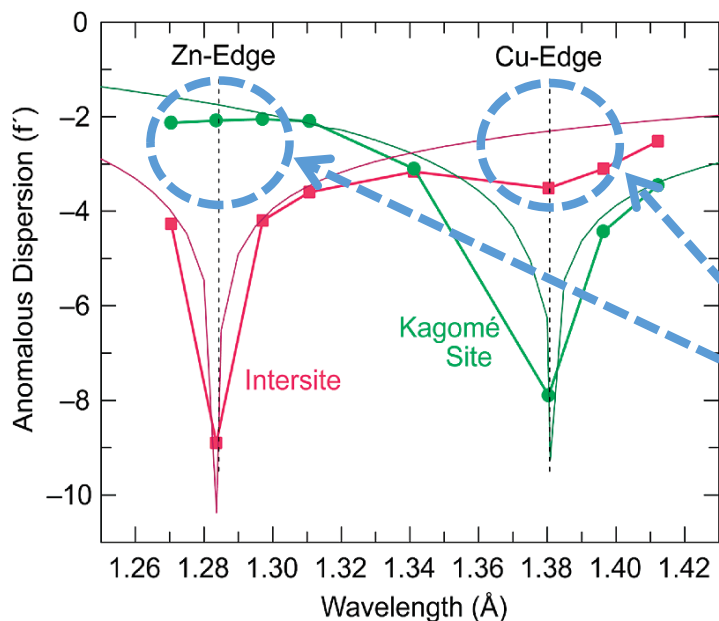
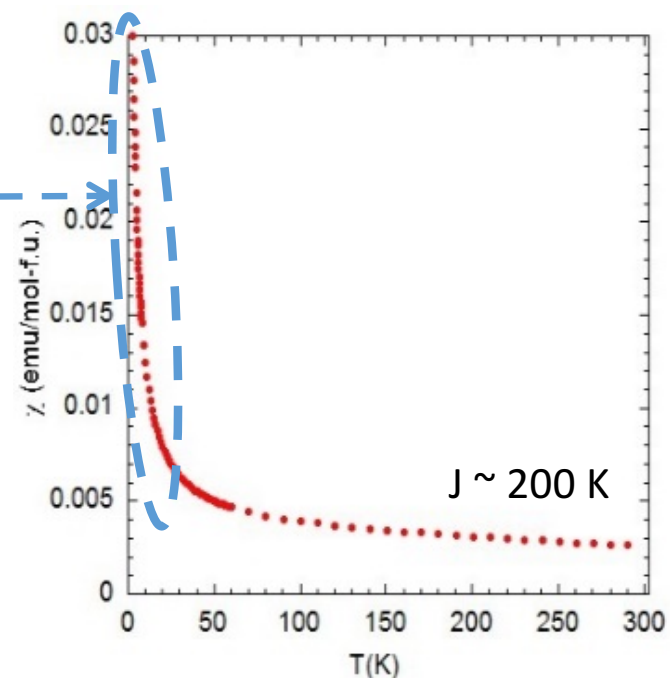
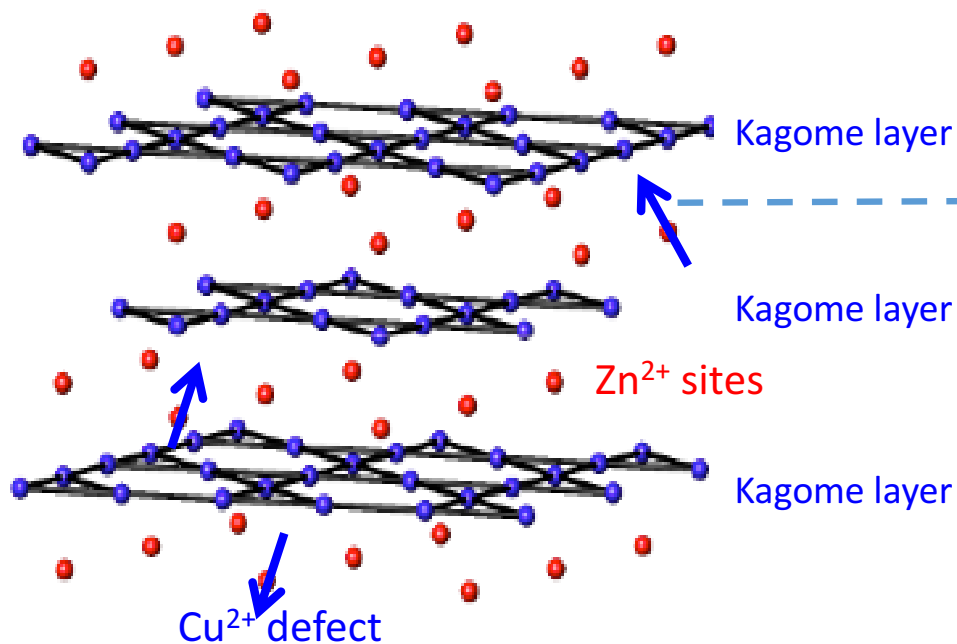
T.-H. Han, *et al.* Nature (2012)

**Good news:** Spinon Continuum (rather than conventional magnon dispersion);  
Consistent with continuous  $S=1/2$  spin excitations from a spin-liquid ground state



**Bad news:** Defect spins dominate the low energy part of spin excitations;  
unable to study the ground state, including the possibility of a small gap

Complications : Defect  $\text{Cu}^{2+}$  spins occupy the non-magnetic  $\text{Zn}^{2+}$  sites with 15% probability  
 $\rightarrow$  actual composition is  $(\text{Zn}_{0.85}\text{Cu}_{0.15})\text{Cu}_3(\text{OH})_6\text{Cl}_2$



$\text{Cu}^{2+}$  defect spins dominate  $\chi$  (and all *bulk-averaged* thermodynamic data) at low temperatures

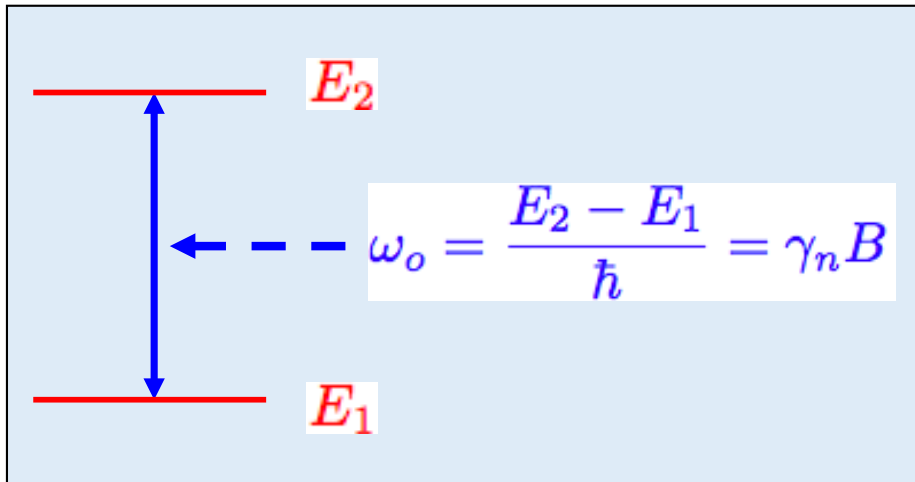
Anomalous X-ray diffraction experiments on single crystal:

- 15% of  $\text{Zn}^{2+}$  sites are occupied by  $\text{Cu}^{2+}$  defect spins
- No  $\text{Zn}^{2+}$  occupy  $\text{Cu}^{2+}$  kagome sites (*i.e.* no anti-site defects)

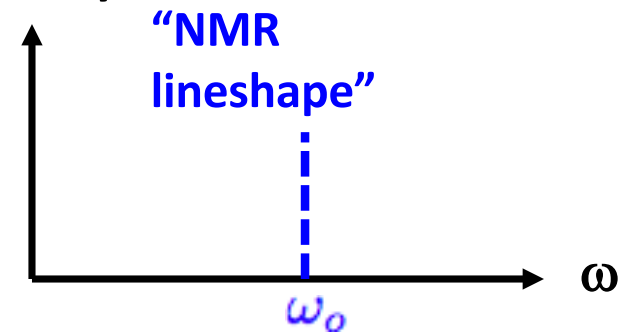
Freedman *et al*, JACS 132 (2010) 16185.

# How shall we probe the properties of the kagome layers separately from the defects?

Answer: NMR

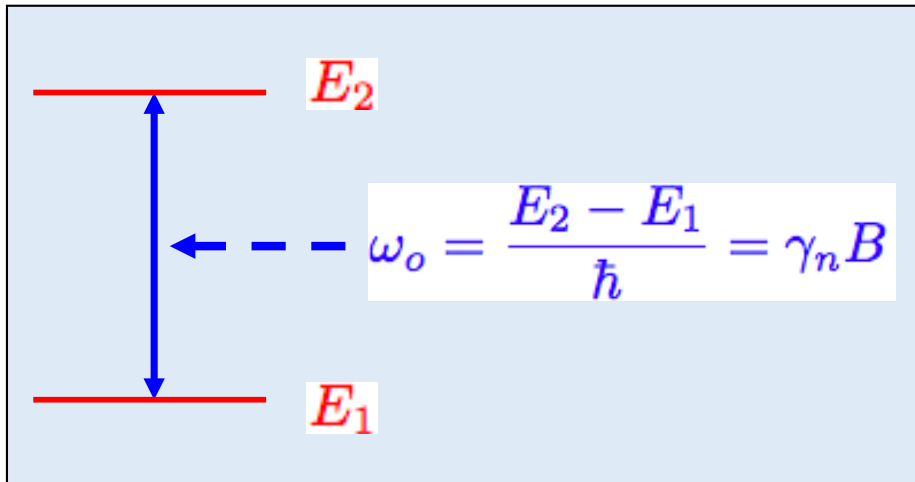


Absorption  
intensity

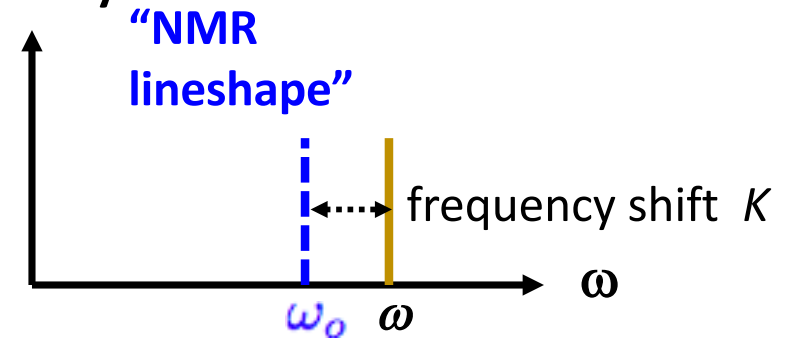


# How shall we probe the properties of the kagome layers separately from the defects?

Answer: NMR

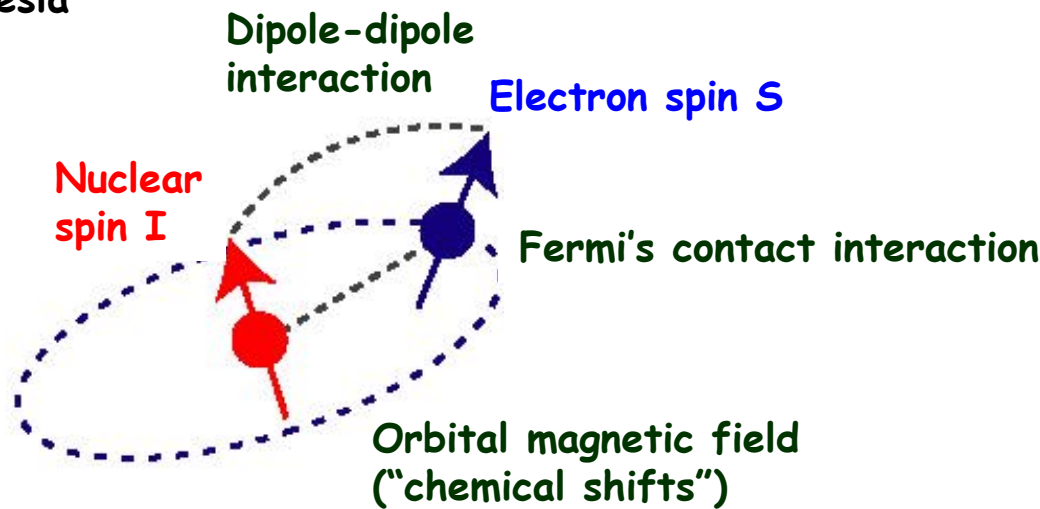


Absorption intensity



## Influence of electron spins via hyperfine interactions

$B_{\text{ext}} \sim 8$  Tesla  
(Zeeman)



NMR frequency shifts to

$$\omega = \gamma_n (B_{\text{ext}} + B_{\text{hf}})$$

$$= \omega_0 (1 + K)$$

$$K = \frac{A_{\text{hf}}}{N_A \mu_B} \chi_{\text{spin}} + K_{\text{chem}}$$

where

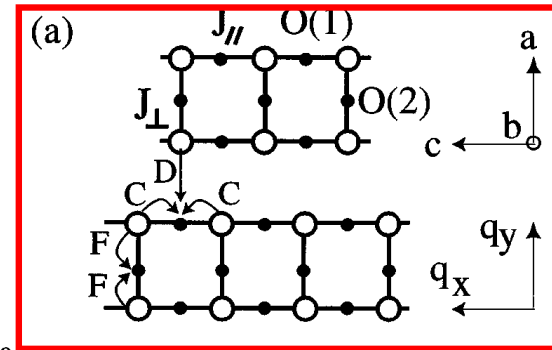
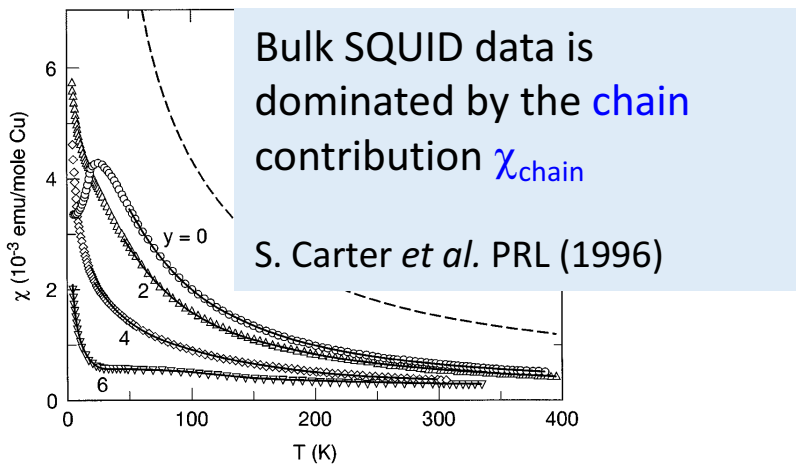
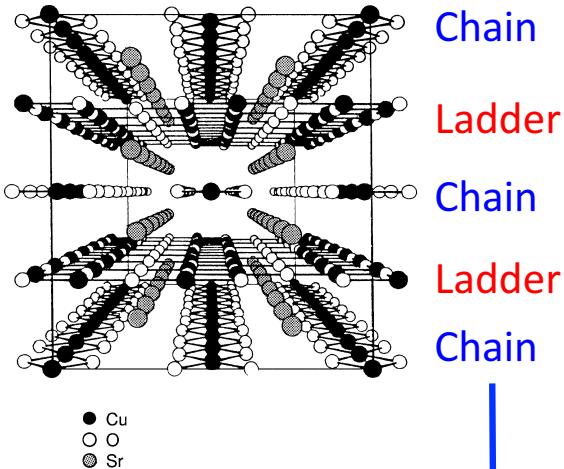
$A_{\text{hf}}$  : "Hyperfine coupling"

$$|K_{\text{chem}}| \sim 0.02(\%) \ll K_{\text{spin}}$$

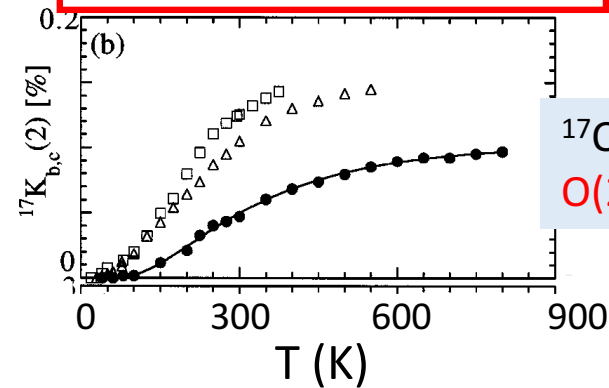


$^{17}\text{O}$  NMR successfully probed a spin liquid state in the two-leg ladder layers of  $\text{A}_{14}\text{Cu}_{24}\text{O}_{41}$   
 although the bulk spin susceptibility is dominated by chain layers !

T. Imai et al., PRL 81 (1998) 220.



Spin liquid on two-leg ladder layer



$^{17}\text{O}$  NMR Knight shift at O(2) sites reflects  $\chi_{\text{Ladder}}$

$^{17}\text{O}$  nuclear spins at O(1) and O(2) sites couple mostly with Cu electron spins in the ladder layers

# First generation $^{63}\text{Cu}$ , $^1\text{H}$ and $^{35}\text{Cl}$ , NMR in partially aligned powder sample of $\text{ZnCu}_3(\text{OH})_6\text{Cl}_2$

T. I. *et al.*, PRL 100 (2008) 077203

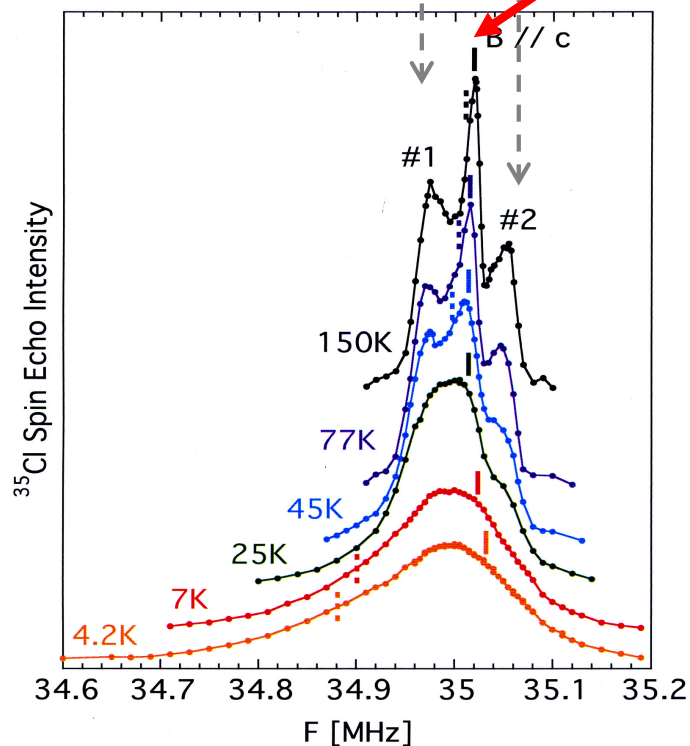
$^{63,65}\text{Cu}$  NMR : Direct but inconvenient probe (nuclear quadrupole interaction too large).

$^1\text{H}$  NMR : hyperfine coupling is too small, compared with line broadening induced by defect spins

$^{35}\text{Cl}$  nuclear spin has decent strength of *negative* hyperfine coupling with Cu electron spins.

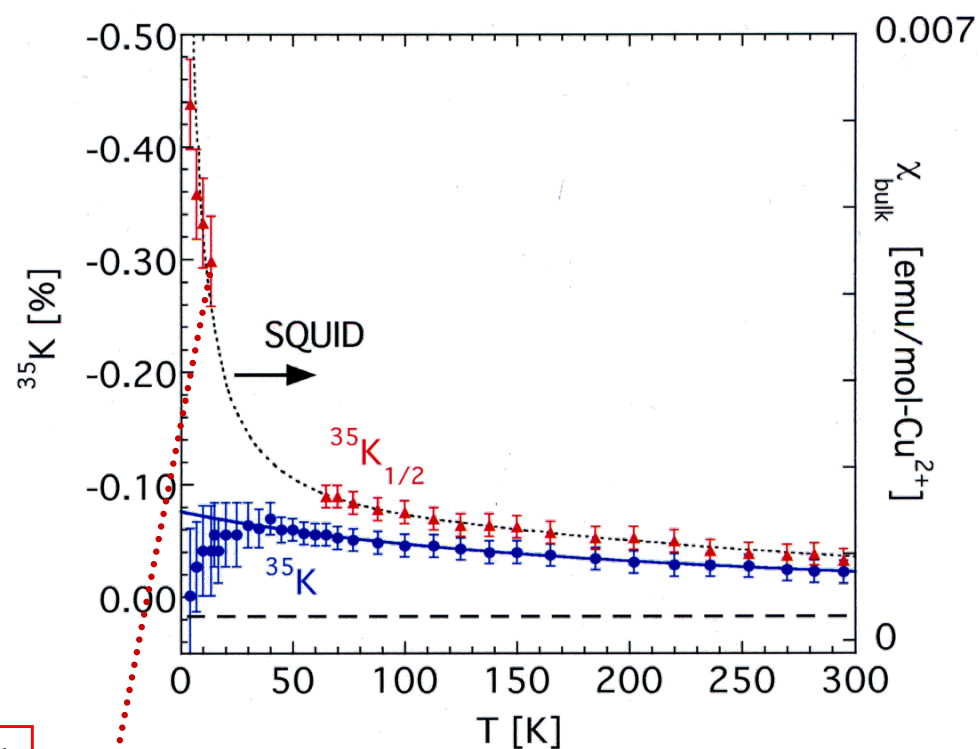
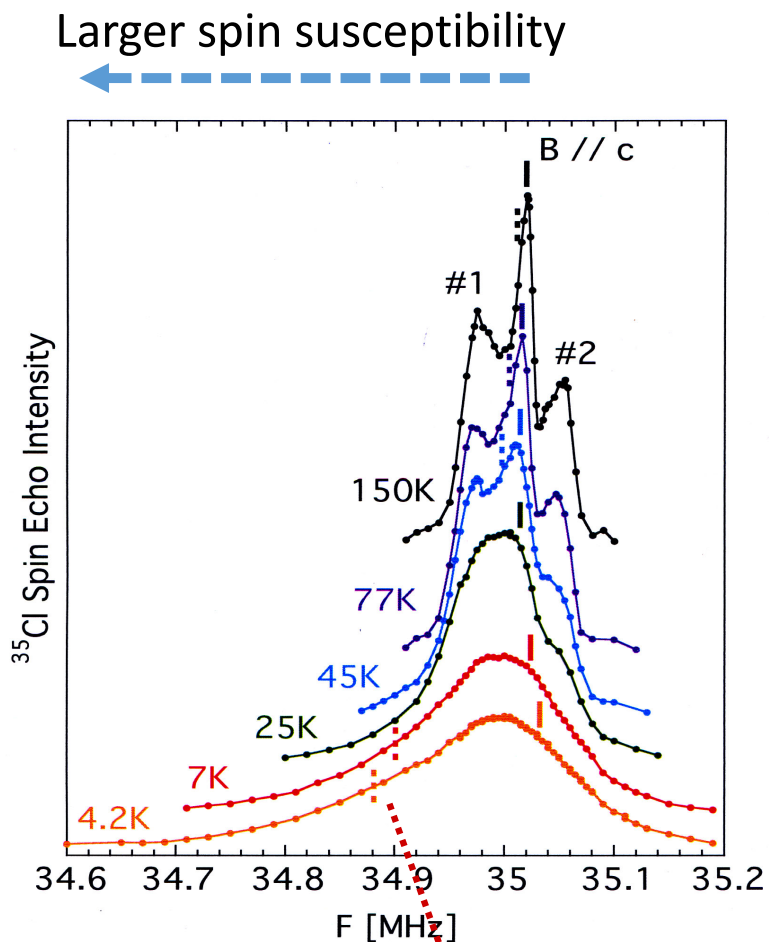
Undesirable shoulders #1 & #2 from other grains split by second order nuclear quadrupole interaction (to be ignored)

Main  $^{35}\text{Cl}$  NMR peak from grains aligned along the c-axis



# $^{35}\text{Cl}$ NMR in partially aligned powder sample of $\text{ZnCu}_3(\text{OH})_6\text{Cl}_2$

T. I. *et al.*, PRL 100 (2008) 077203

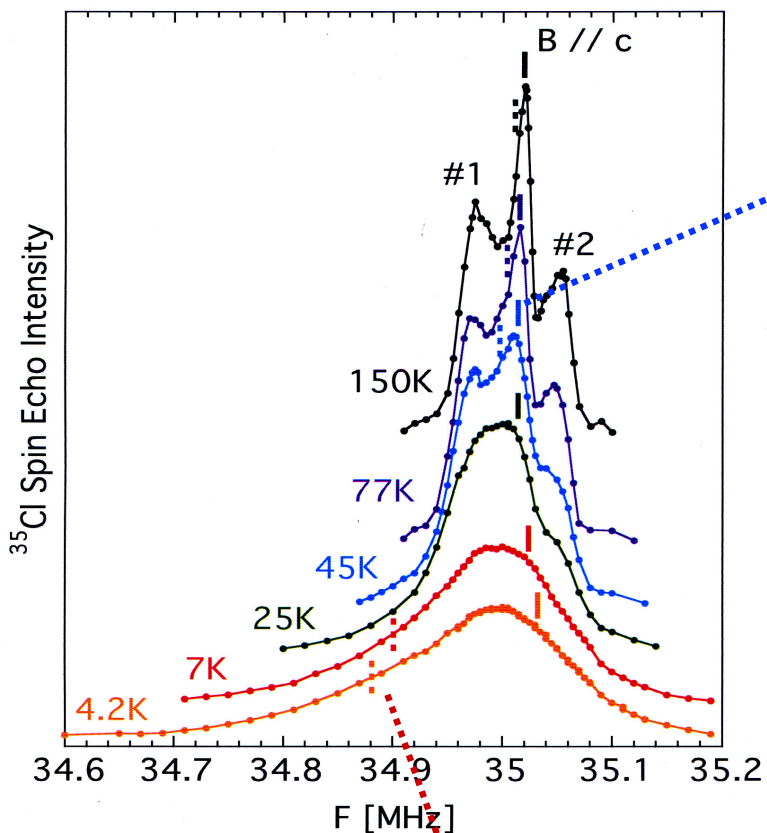


Asymmetrically broadened. Low frequency tail reflects large Curie-Weiss defect susceptibility.

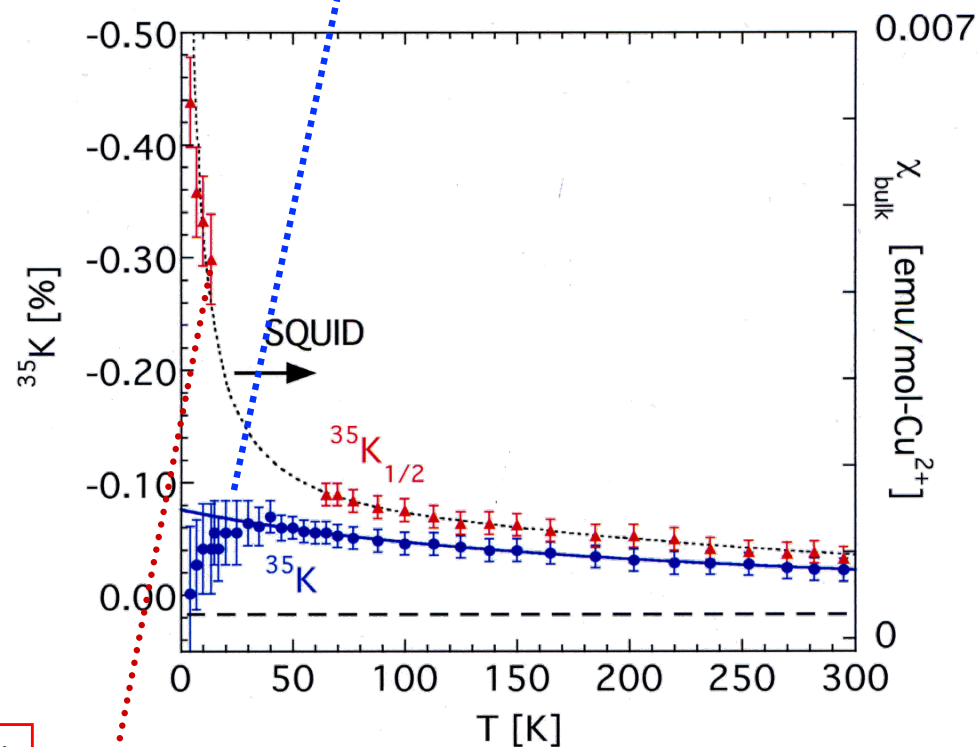
# $^{35}\text{Cl}$ NMR in partially aligned powder sample of $\text{ZnCu}_3(\text{OH})_6\text{Cl}_2$

T. I. et al., PRL 100 (2008) 077203

Larger spin susceptibility

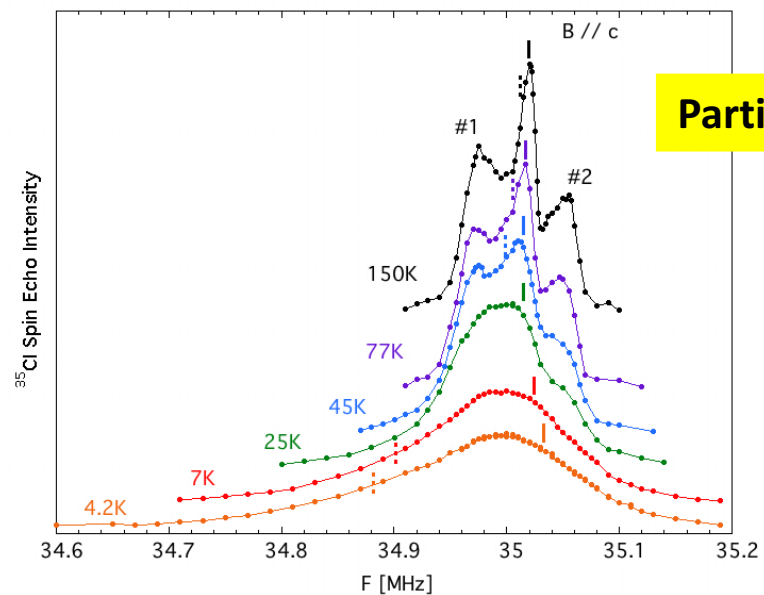


Main peak seems to suggest  $\chi_{\text{kagome}} \rightarrow 0$  at  $T = 0$ , but inconclusive

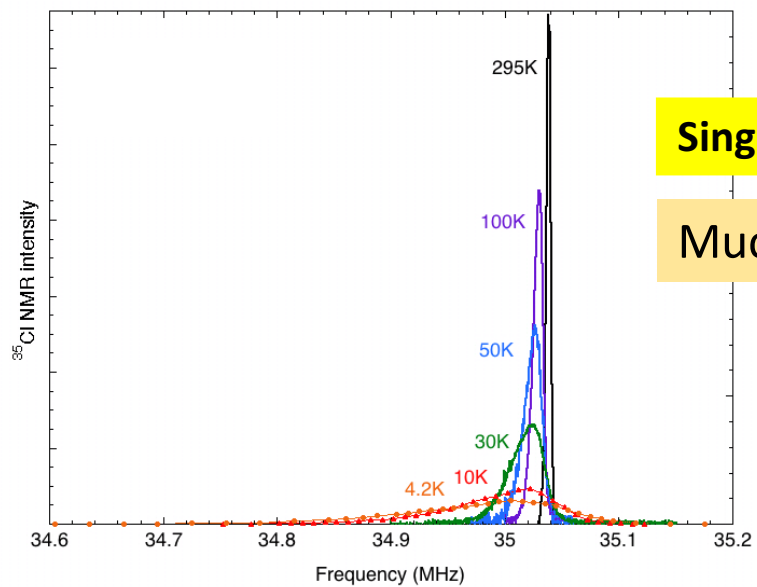


Asymmetrically broadened. Low frequency tail reflects large Curie-Weiss defect susceptibility.

# Advantages of single crystal NMR of $\text{ZnCu}_3(\text{OH})_6\text{Cl}_2$



Partially aligned powder



Single crystal (B || c)

Much higher resolutions!

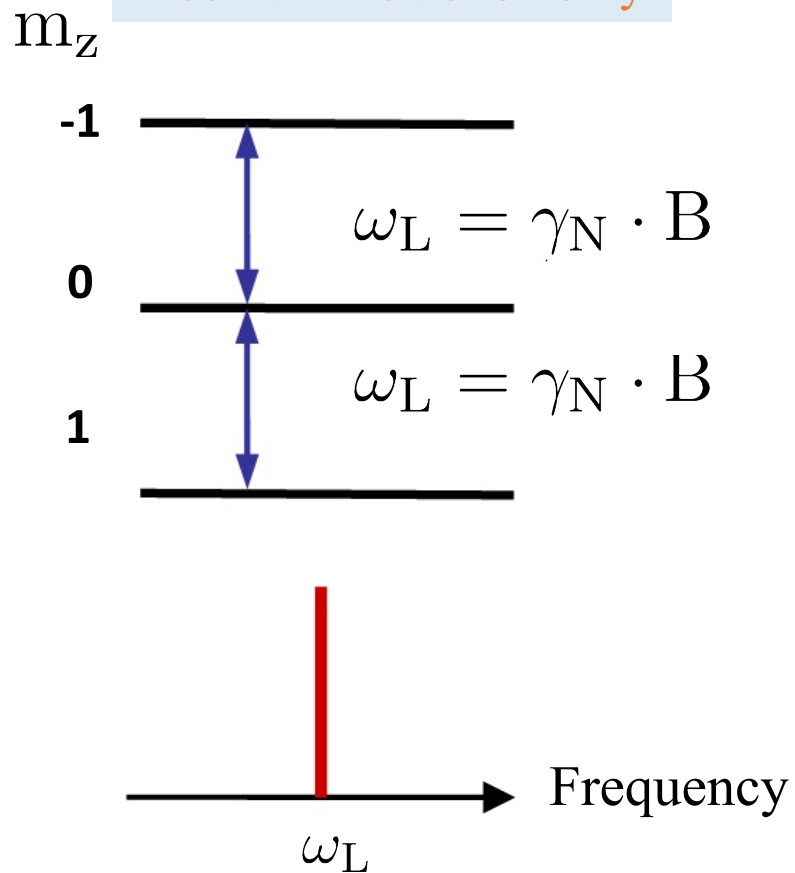
# Second generation $^2\text{D}$ (nuclear spin $I = 1$ ) NMR in $\text{ZnCu}_3(\text{OD})_6\text{Cl}_2$

## deuterated single crystal

T. I. *et al.*, PRB 83(2011) 020411 (Rapid).

$$H = -\gamma_n \hbar \mathbf{B} \cdot \mathbf{I}$$

Zeeman interaction only



# Second generation $^2\text{D}$ (nuclear spin $I = 1$ ) NMR in $\text{ZnCu}_3(\text{OD})_6\text{Cl}_2$

## deuterated single crystal

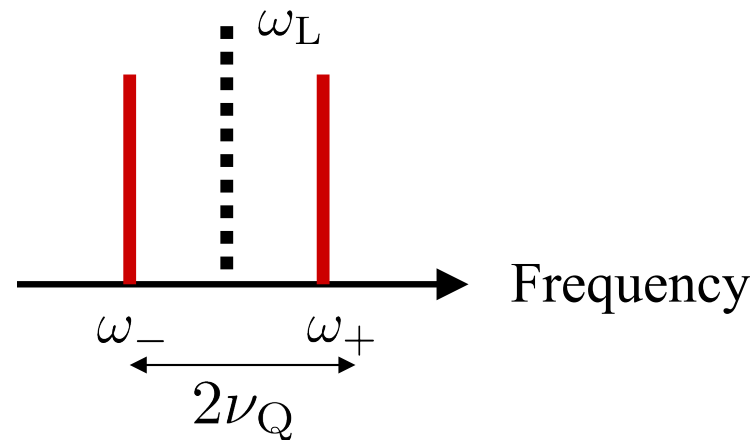
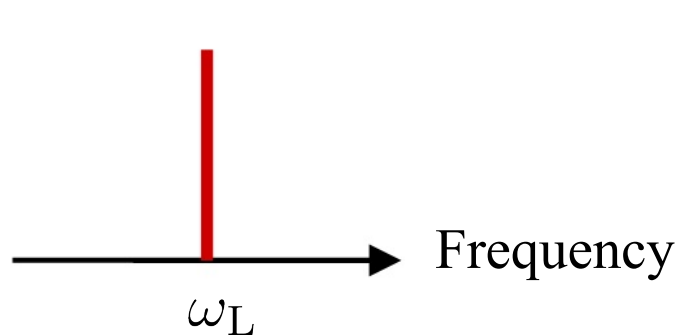
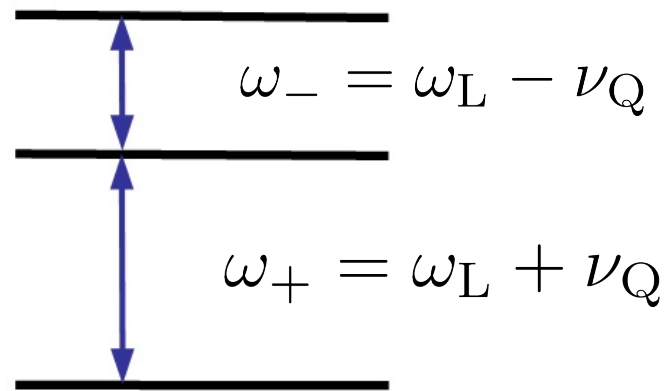
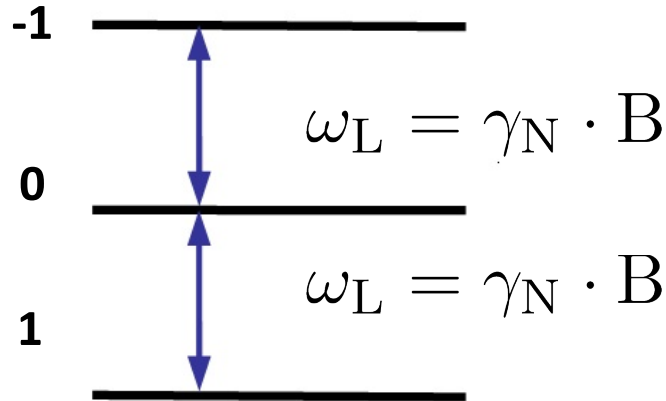
T. I. et al., PRB 83(2011) 020411 (Rapid).

$$H = -\gamma_n \hbar \mathbf{B} \cdot \mathbf{I} + \frac{\hbar \nu_Q^Z}{6} \{3I_z^2 - I(I+1) + \eta(I_x^2 - I_y^2)\}$$

Zeeman interaction only

Nuclear quadrupole interaction with charge/lattice

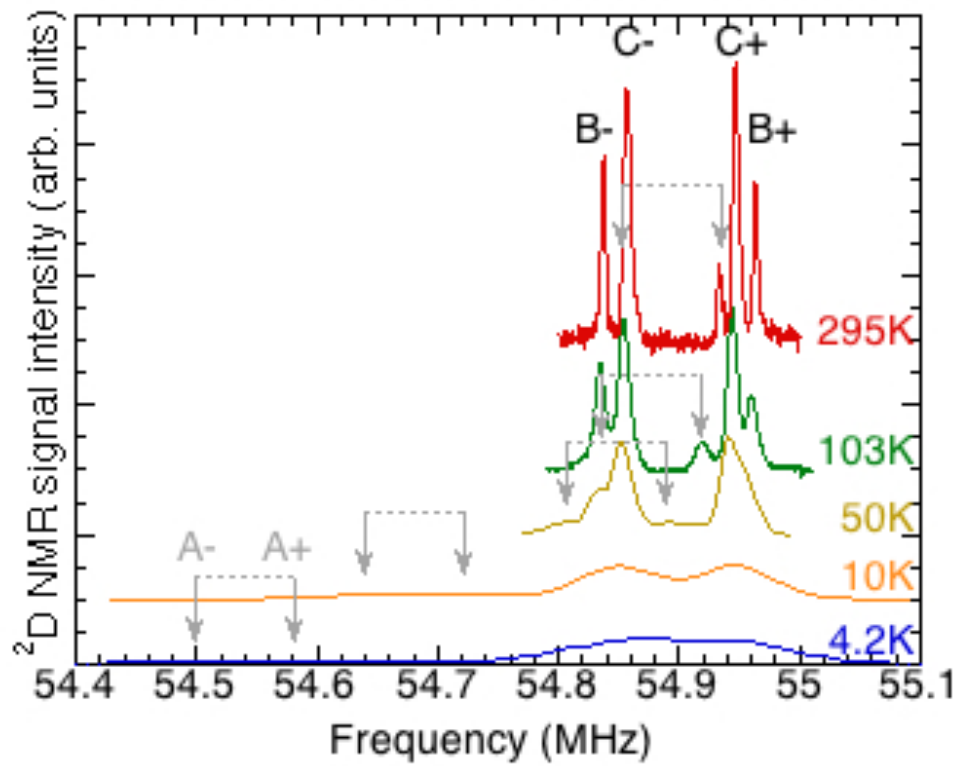
$m_z$



# $^2\text{D}$ single crystal NMR revealed 14% $\text{Zn}^{2+}$ sites are occupied by $\text{Cu}^{2+}$ defects in $\text{ZnCu}_3(\text{OD})_6\text{Cl}_2$

## 3 pairs of $^2\text{D}$ NMR signals from 3 inequivalent $^2\text{D}$ sites

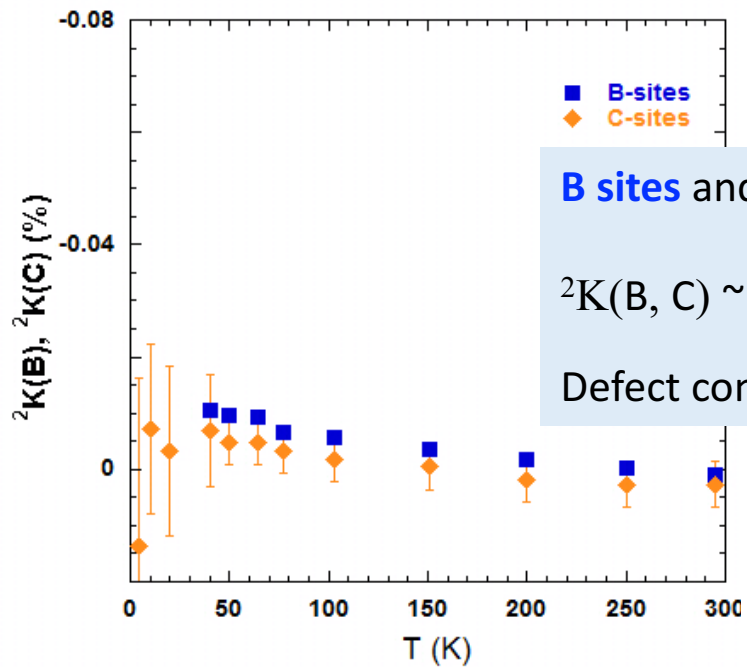
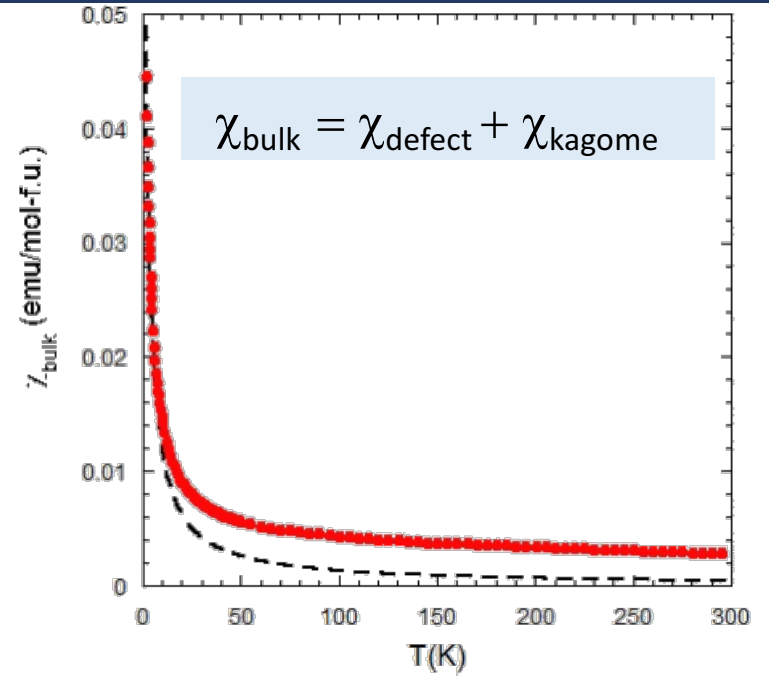
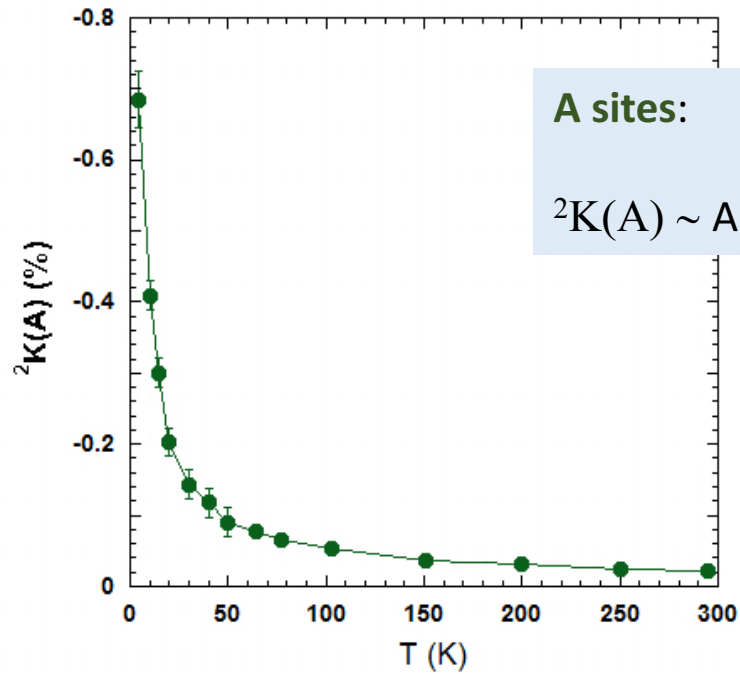
- A sites** (~14% population) : **NN of  $\text{Cu}^{2+}$  defects** occupying  $\text{Zn}^{2+}$  non-magnetic sites.
- B sites** (~28% population) : **NNN of  $\text{Cu}^{2+}$  defects** occupying  $\text{Zn}^{2+}$  non-magnetic sites
- C sites** (~58% population) : **No defects nearby**



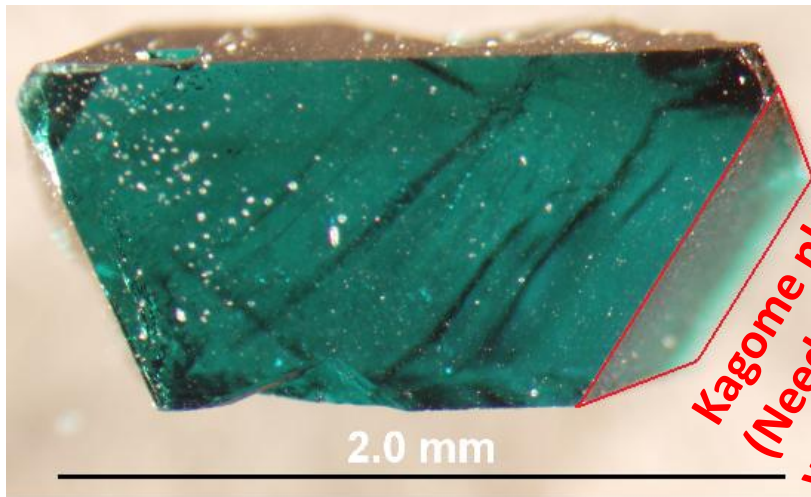
Consistent with  $\text{Zn}_{0.86}\text{Cu}_{3.14}(\text{OD})_6\text{Cl}_2$ ;  
~14% of  $\text{Zn}^{2+}$  sites are occupied by  $\text{Cu}^{2+}$  defect spins

No evidence for anti-site  $\text{Zn}^{2+}$  defects occupying  $\text{Cu}^{2+}$  sites

# Defect spin susceptibility probed by $^2\text{D}$ A sites in $\text{ZnCu}_3(\text{OD})_6\text{Cl}_2$



# Change of strategy: angle-dependent $^{17}\text{O}$ (nuclear spin $I = 5/2$ ) NMR for isotope-enriched single crystal



*Kagome plane  
(Need to be aligned  
with magnetic field)*

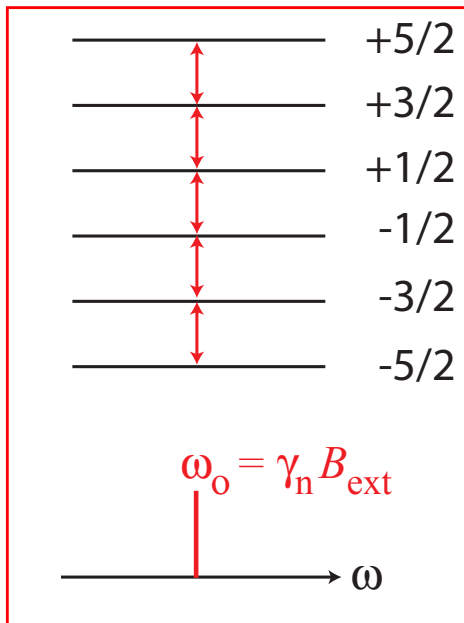


Single crystal courtesy of T.-H. Han & Y.S. Lee

Compact goniometer for NMR & X-ray designed by M. Fu

# Nuclear spin Hamiltonian for $^{17}\text{O}$ (nuclear spin $I = 5/2$ ) and resonant peak(s)

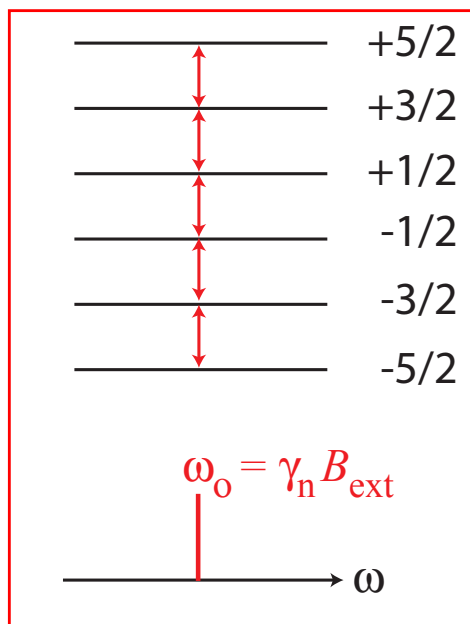
$$\hat{H} = \gamma_n \vec{B}_{ext} \cdot \vec{I}$$



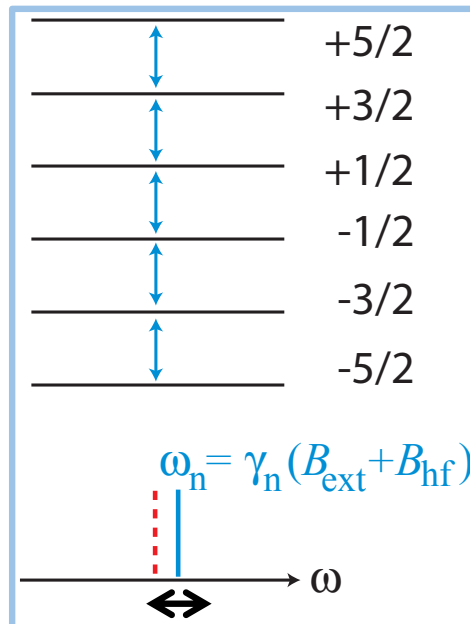
Zeeman only

# Nuclear spin Hamiltonian for $^{17}\text{O}$ (nuclear spin $I = 5/2$ ) and resonant peak(s)

$$\hat{H} = \gamma_n \vec{B}_{ext} \cdot \vec{I} + \gamma_n \vec{B}_{hf} \cdot \vec{I}$$



Zeeman only



Zeeman + hyperfine

NMR frequency shifts to

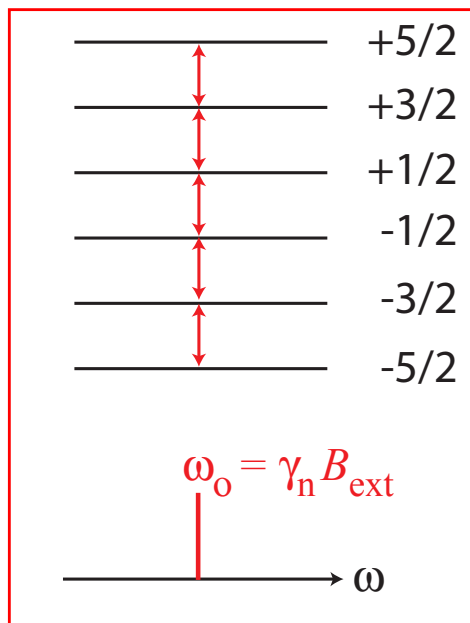
$$\omega_n = \omega_0(1 + K)$$

where 
$$K = \frac{A_{hf}}{N_A \mu_B} \chi_{spin} + K_{chem}$$

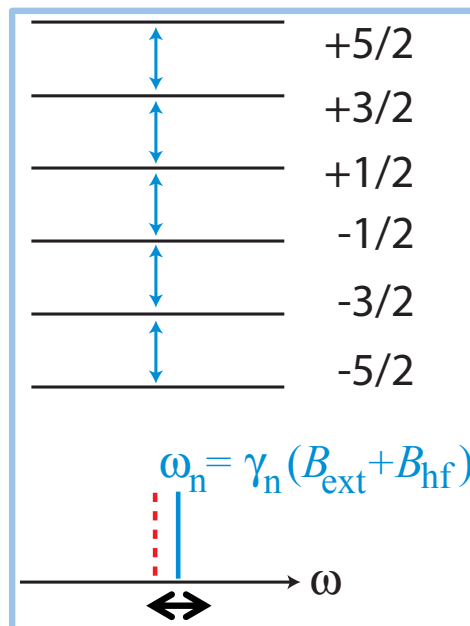
and  $|K_{chem}| \sim 0.02(\%) \ll K_{spin}$

# Nuclear spin Hamiltonian for $^{17}\text{O}$ (nuclear spin $I = 5/2$ ) and resonant peak(s)

$$\hat{H} = \boxed{\gamma_n \vec{B}_{ext} \cdot \vec{I}} + \boxed{\gamma_n \vec{B}_{hf} \cdot \vec{I}} + \boxed{\frac{\nu_Q}{2} \hat{I}_z^2} + \dots$$



Zeeman only



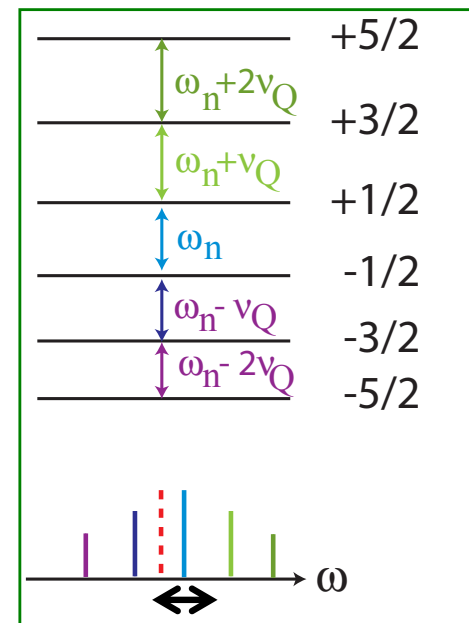
Zeeman + hyperfine

NMR frequency shifts to

$$\omega_n = \omega_0(1 + K)$$

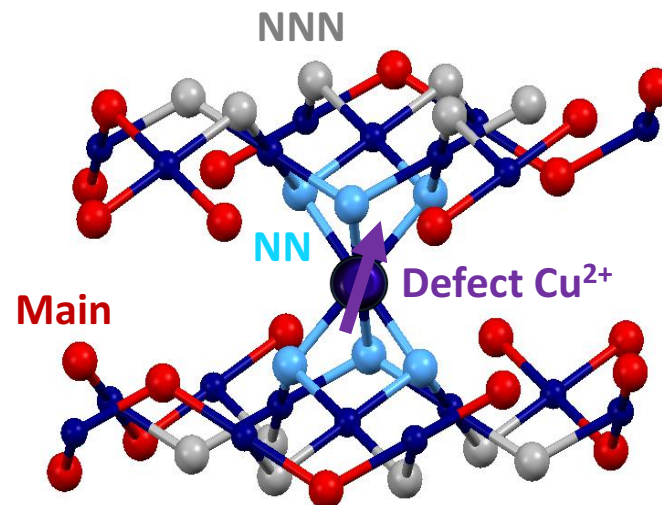
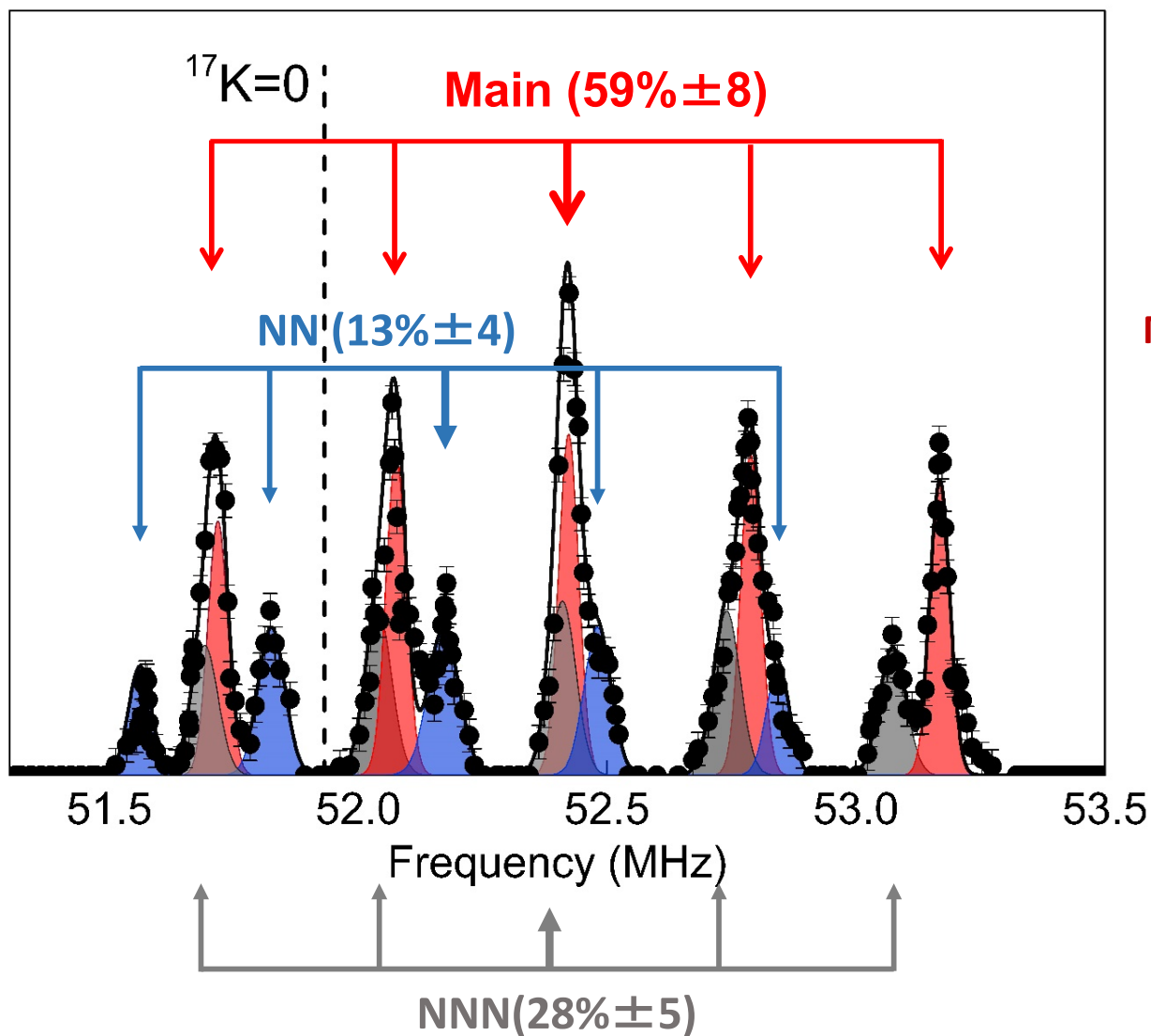
$$\text{where } K = \frac{A_{hf}}{N_A \mu_B} \chi_{spin} + K_{chem}$$

and  $|K_{chem}| \sim 0.02(\%) \ll K_{spin}$



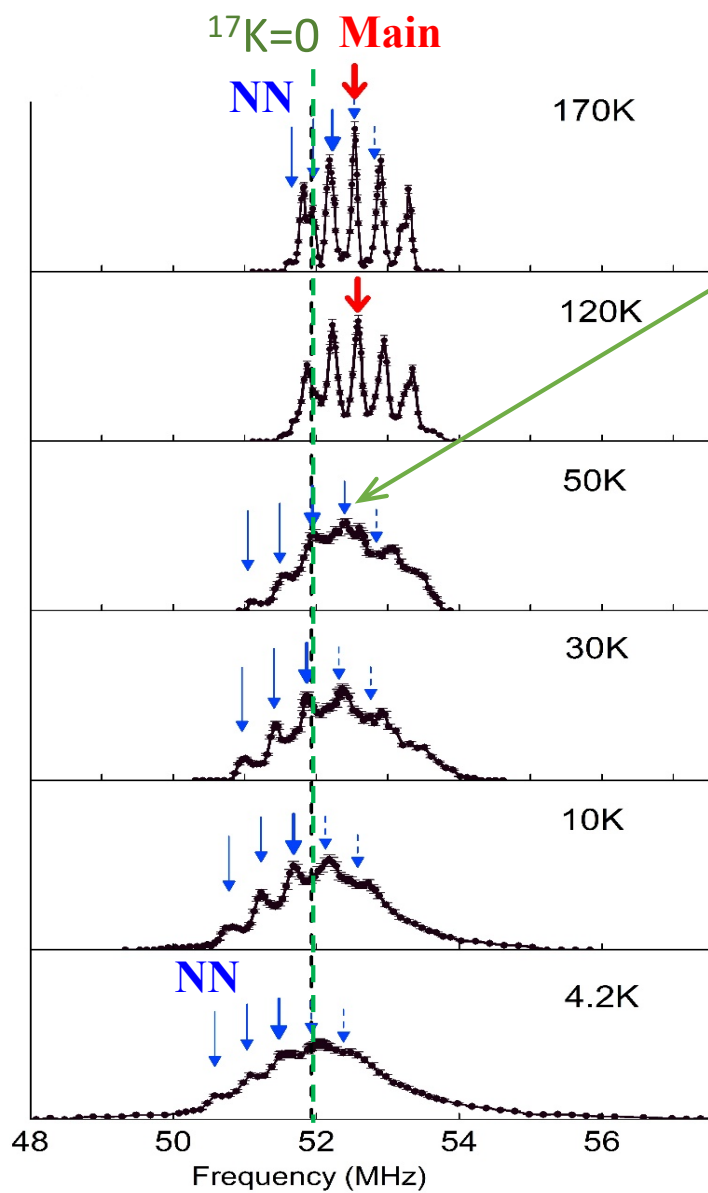
Zeeman + hyperfine + quadrupole interaction

# $^{17}\text{O}$ NMR lineshape of $\text{ZnCu}_3(\text{OH})_6\text{Cl}_2$ single crystal in $B_{\text{ext}} \parallel c$



# Temperature dependence of $^{17}\text{O}$ NMR lineshapes in $B_{\text{ext}} \parallel c$

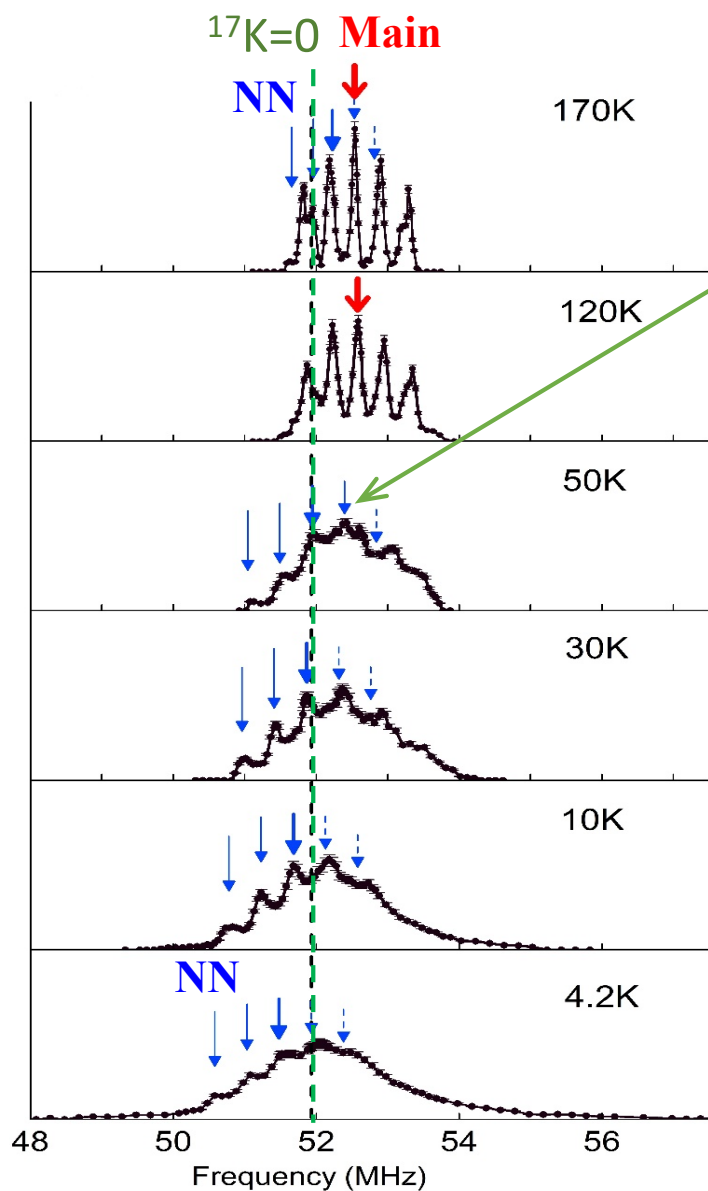
M Fu *et al.* Science (2015)



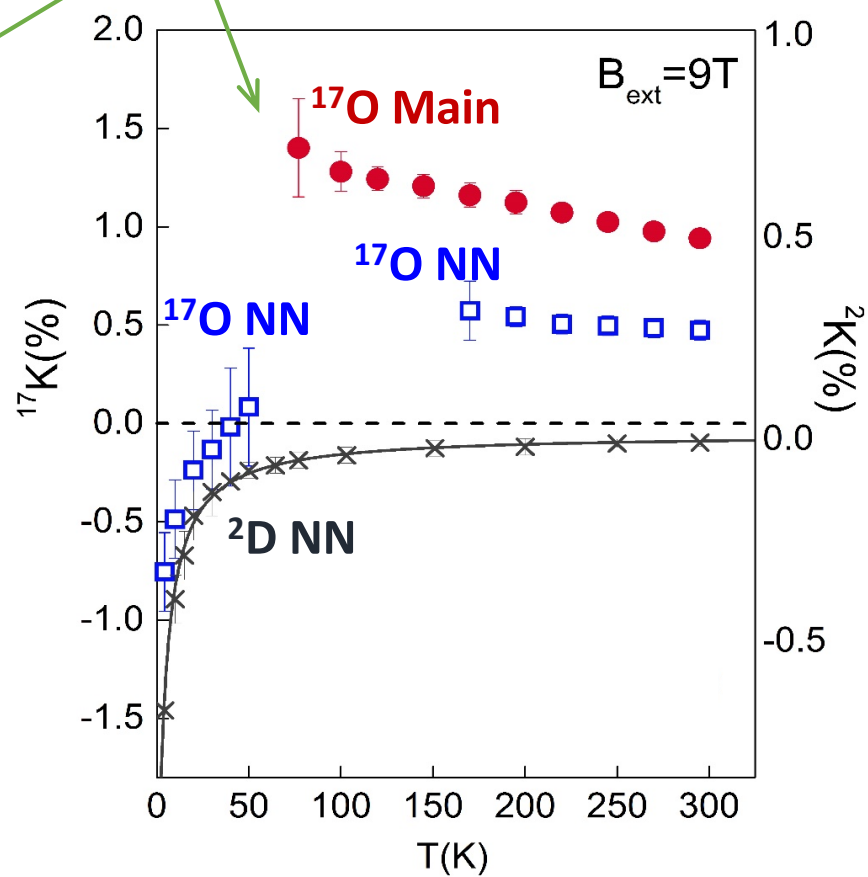
We cannot resolve the crucial center peak of the **Main sites** below  $\sim 50\text{K}$

# Temperature dependence of $^{17}\text{O}$ NMR lineshapes in $B_{\text{ext}} \parallel c$

M. Fu *et al.* Science (2015)

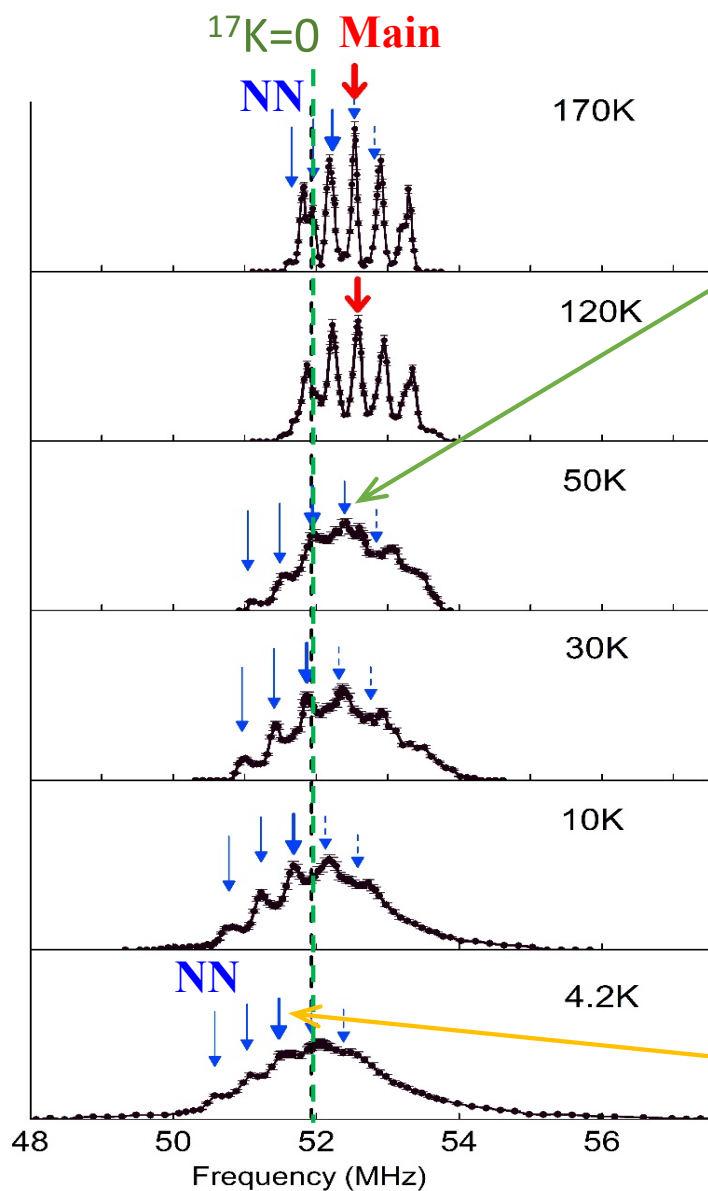


We cannot resolve the crucial center peak of the **Main sites** below  $\sim 50\text{K}$

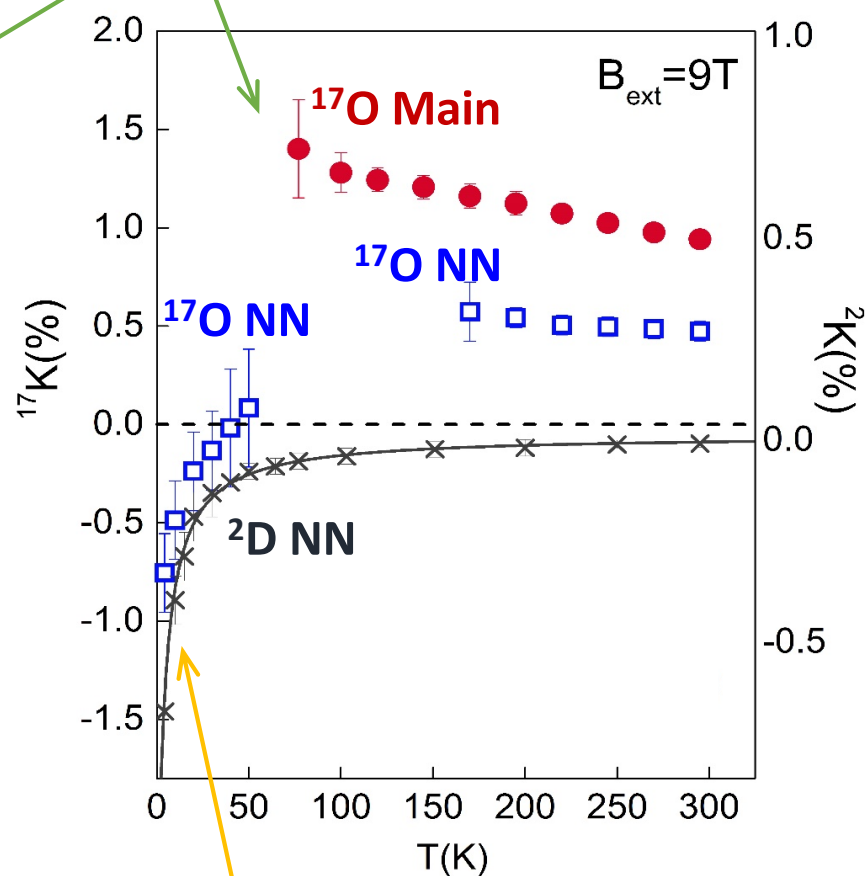


# Temperature dependence of $^{17}\text{O}$ NMR lineshapes in $B_{\text{ext}} \parallel c$

Fu *et al.* Science (2015)



We cannot resolve the crucial center peak of the **Main sites** below  $\sim 50\text{K}$



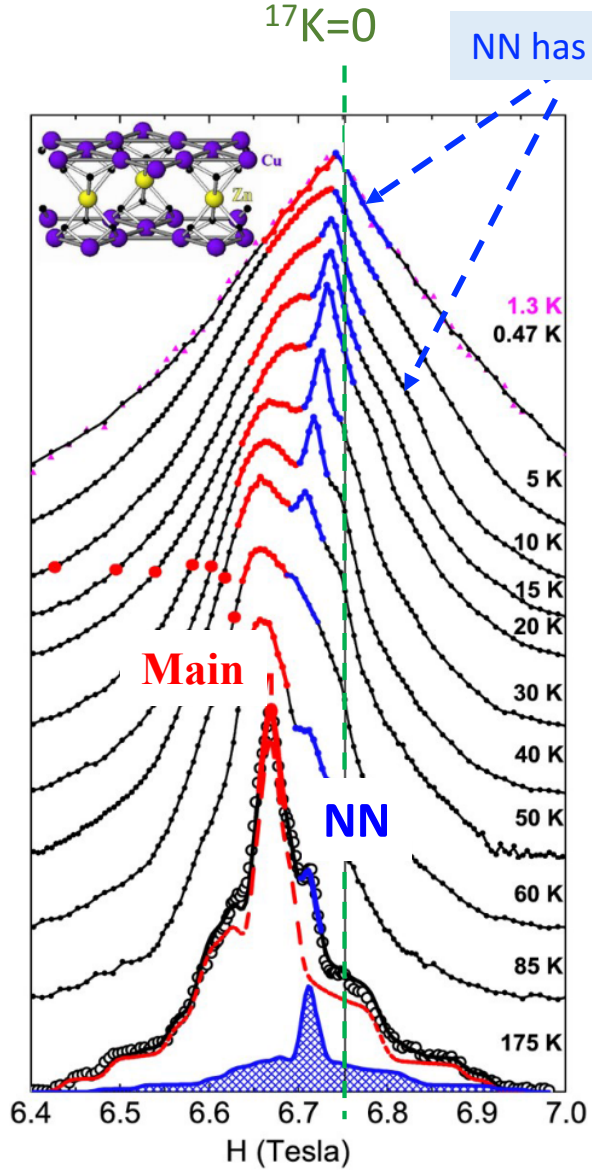
Low T behavior at  $^{17}\text{O}$  and  $^{2}\text{D}$  NN sites is dominated by a large Curie - Weiss contribution,

$$\chi_{\text{defect}} \sim \frac{C}{T + \theta}$$

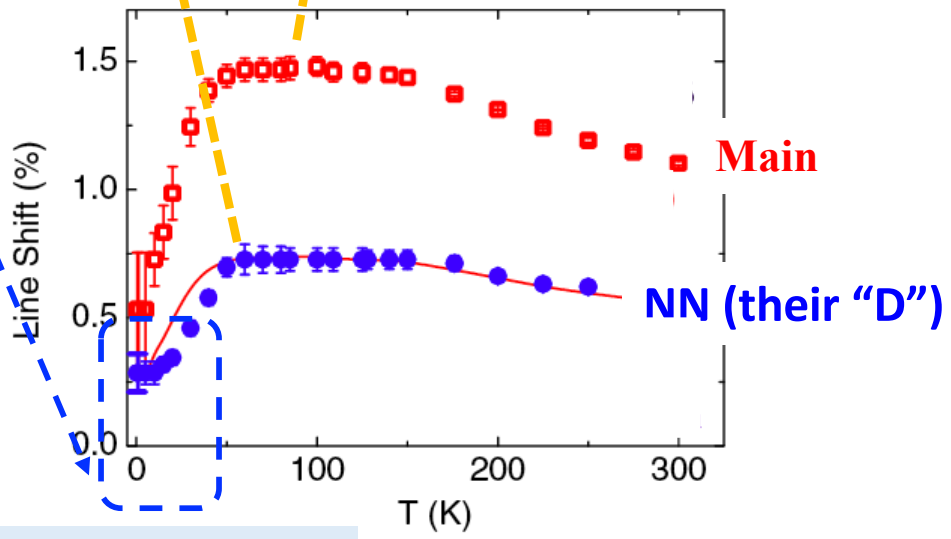
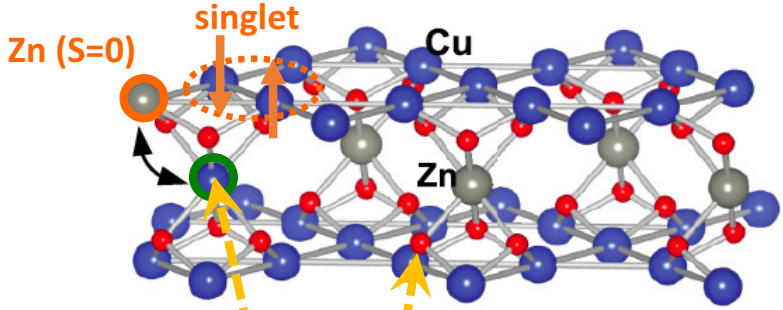
with  $\theta \sim 1$  K and negative hyperfine coupling  $A_{\text{hf}} < 0$

(Side) Earlier powder  $^{17}\text{O}$  results are consistent with our data (NOT a proof of anti-site defects)

Olariu, Mendels *et al.*, PRL 100 (2008) 087202



NN has negative shifts at low T

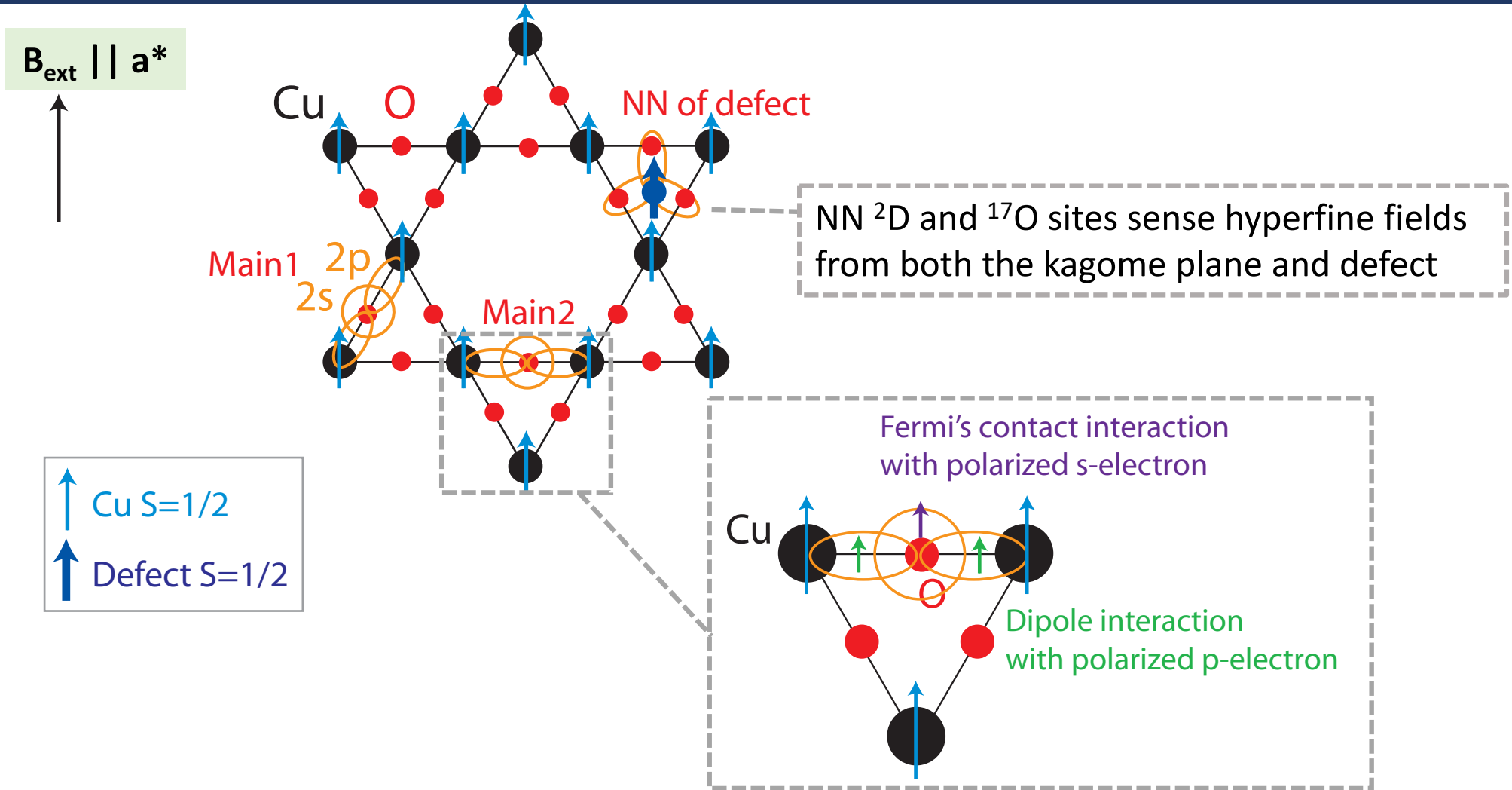


NN data points should have been negative

← Positive shift (in field swept mode)

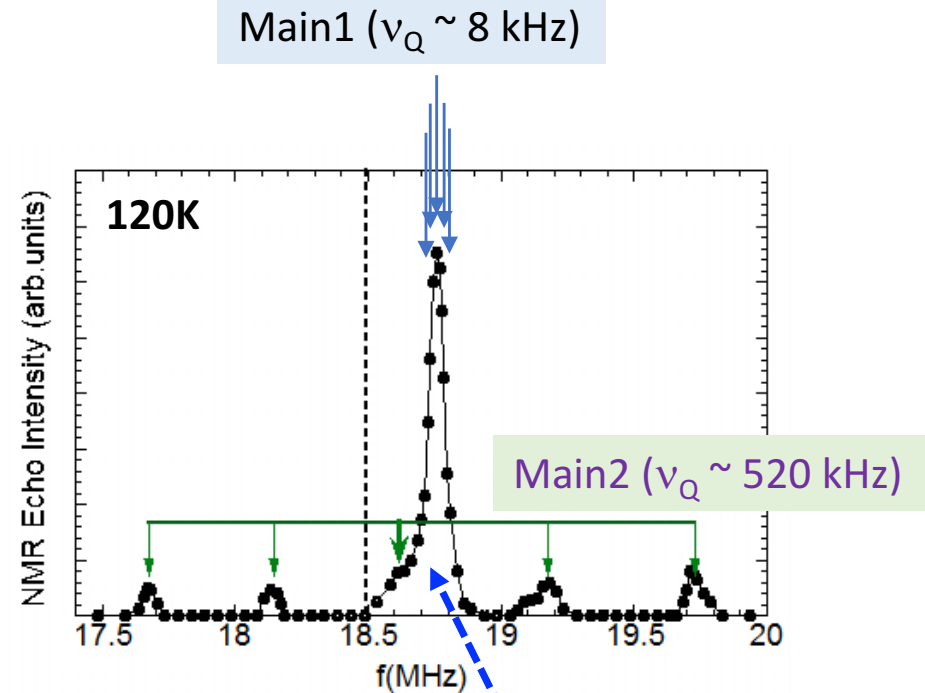
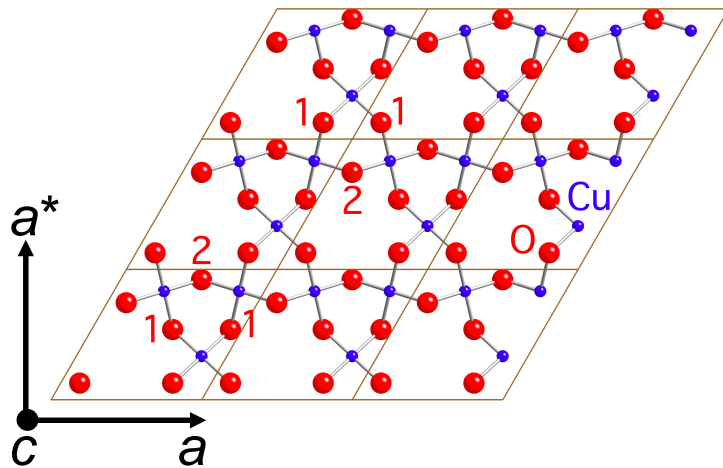
Try a different field geometry :  $B_{\text{ext}} \parallel a^*$

(which we initially thought would be hopelessly complicated)



- Hybridization between O 2s & 2p orbitals and Cu 3d orbital(s) transfers spin polarization to O sites.
- The latter interacts with the  $^{17}\text{O}$  nuclear spin.
- *Main1, Main2, NN sites have different hyperfine fields from Cu sites, hence each of 5 NMR transitions split*

# Intrinsic susceptibility $\chi_{\text{kagome}}$ of the kagome plane as determined from the $^{17}\text{O}$ Knight shift in $B = 3.2 \text{ T} \parallel a^*$



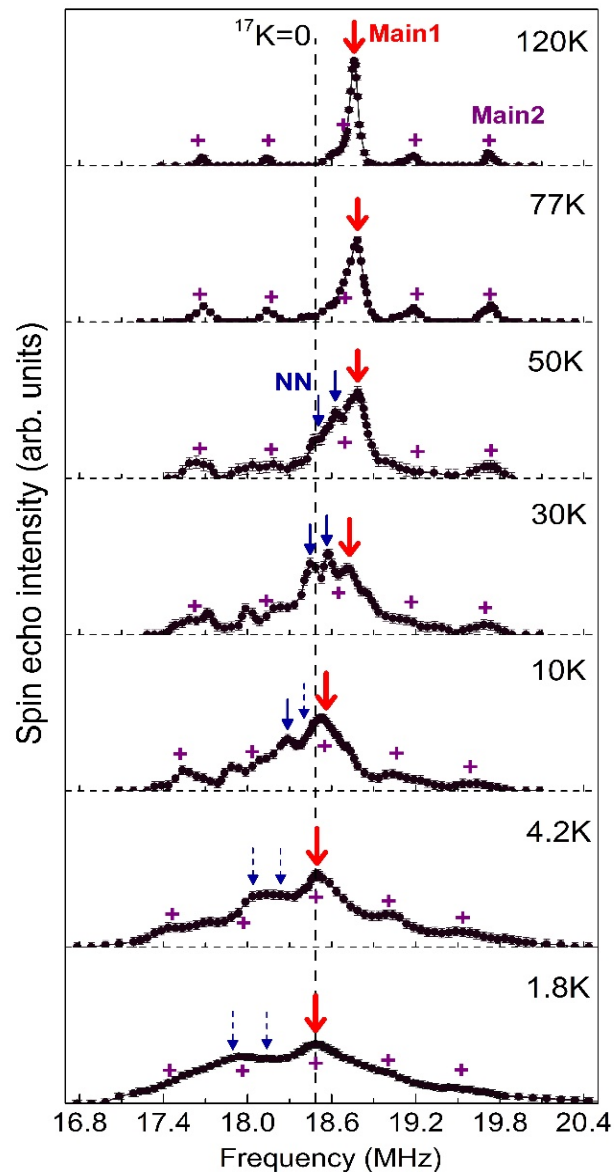
Hyperfine tensors depend on the relative orientation of the magnetic field  $B$  with respect to the Cu-O-Cu bond axis.



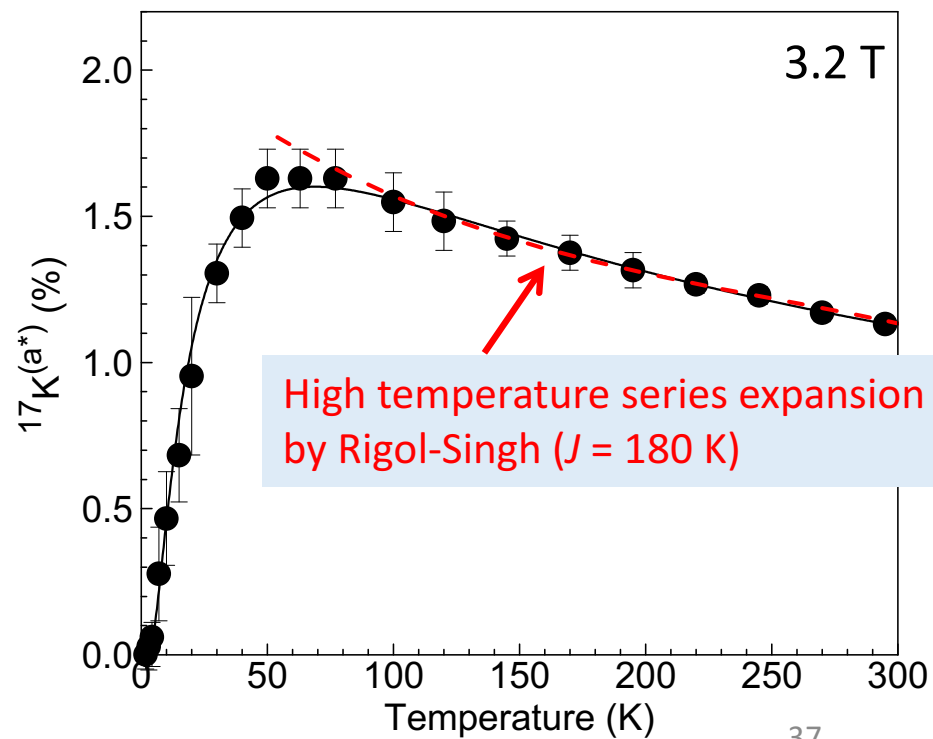
$^{17}\text{O}$  NMR signals at “**Main1**” and “**Main2**” sites appear separately with the intensity ratio  $\sim 2 : 1$ .

“**Main1**” sites happen to have  $\nu_Q \sim 0$  for  $B \parallel a^*$ . All 5 transitions appear together as a **gigantic peak!!**

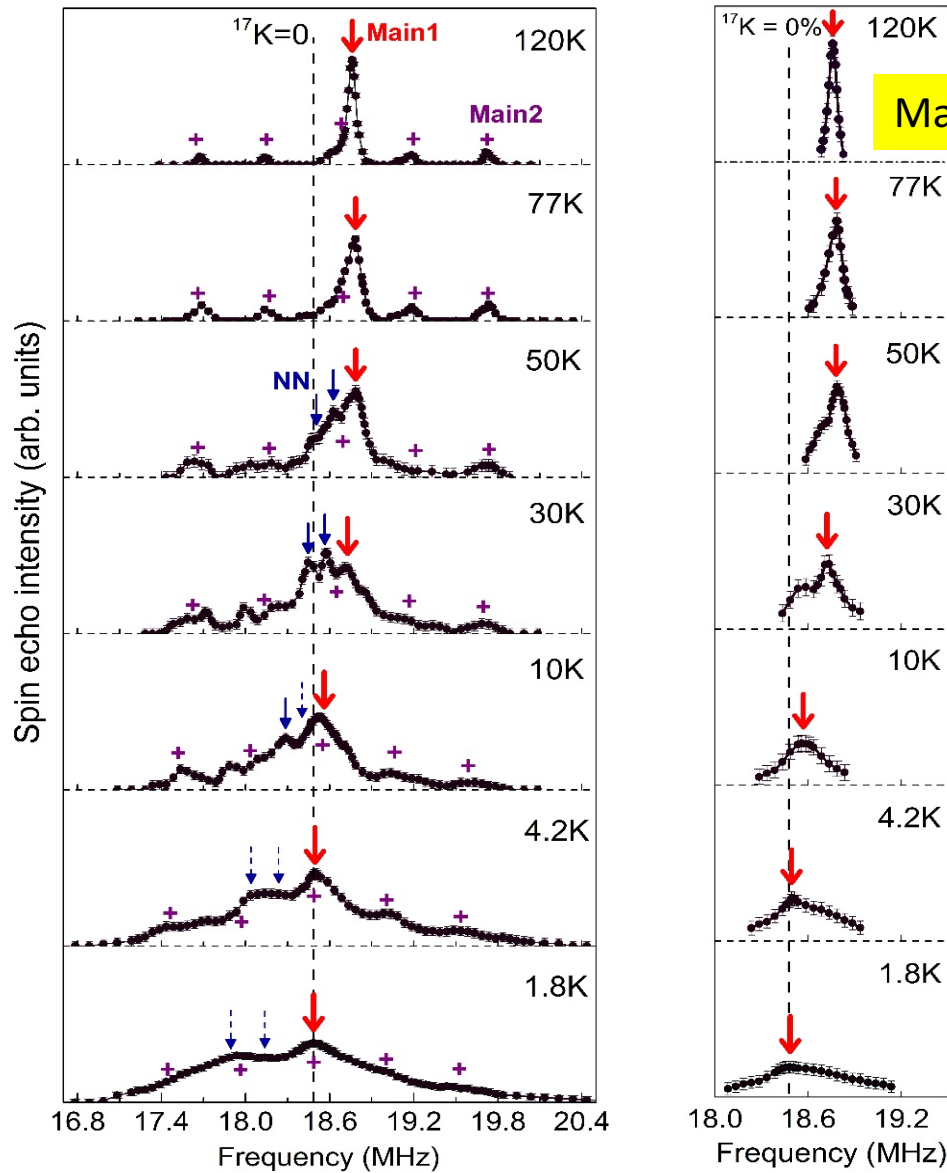
# Intrinsic susceptibility $\chi_{\text{kagome}}$ of the kagome plane as determined from the $^{17}\text{O}$ Knight shift at the main sites measured with $B = 3.2 \text{ T} \parallel a^*$



  
 Larger frequency shift  
 Larger  $^{17}\text{K}$  and  $\chi_{\text{kagome}}$



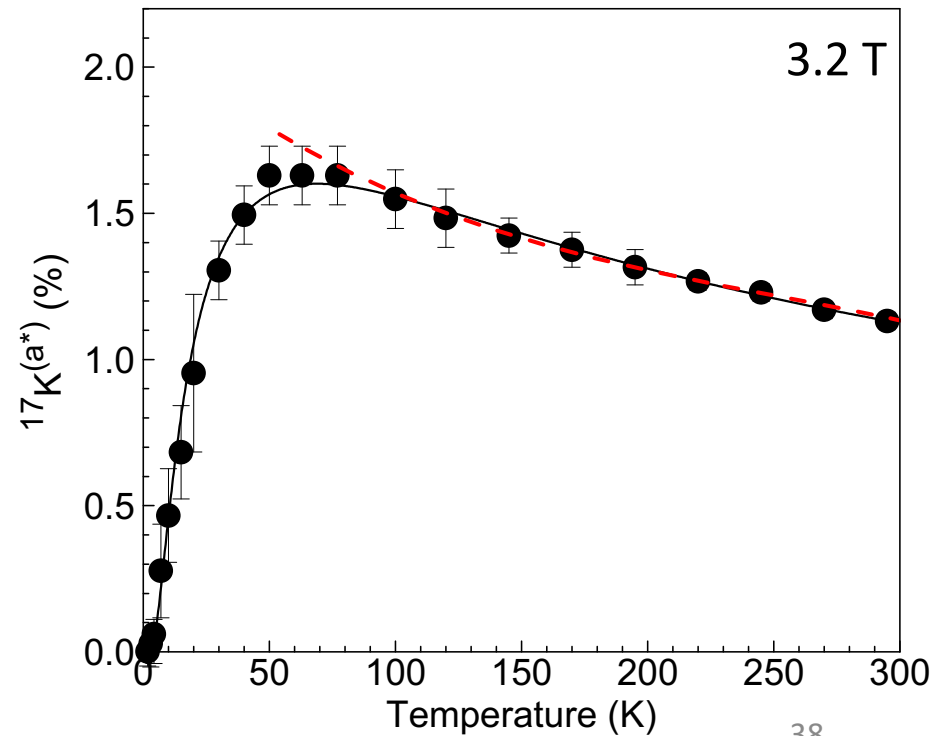
# Intrinsic susceptibility $\chi_{\text{kagome}}$ of the kagome plane as determined from the $^{17}\text{O}$ Knight shift at the main sites measured with $B = 3.2 \text{ T} \parallel a^*$



Main1 only (measured with long RF pulses)

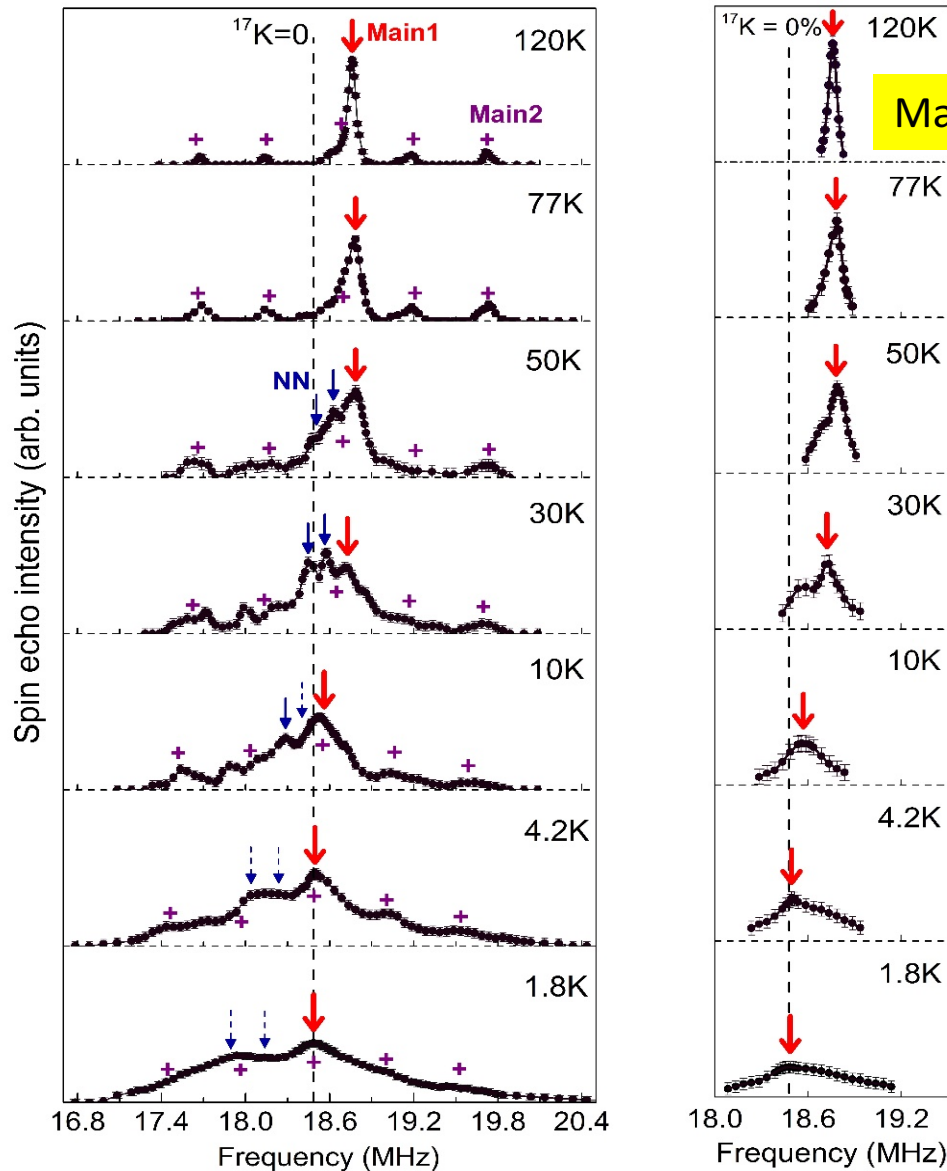
The optimal RF pulse width for Main1 is factor 2 ~ 3 times broader (because we flip all 5 transitions at the same time).

We can measure Main1 peak **selectively**, and observed the same results for  $^{17}\text{K}$ .



→ Larger frequency shift  
Larger  $^{17}\text{K}$  and  $\chi_{\text{kagome}}$

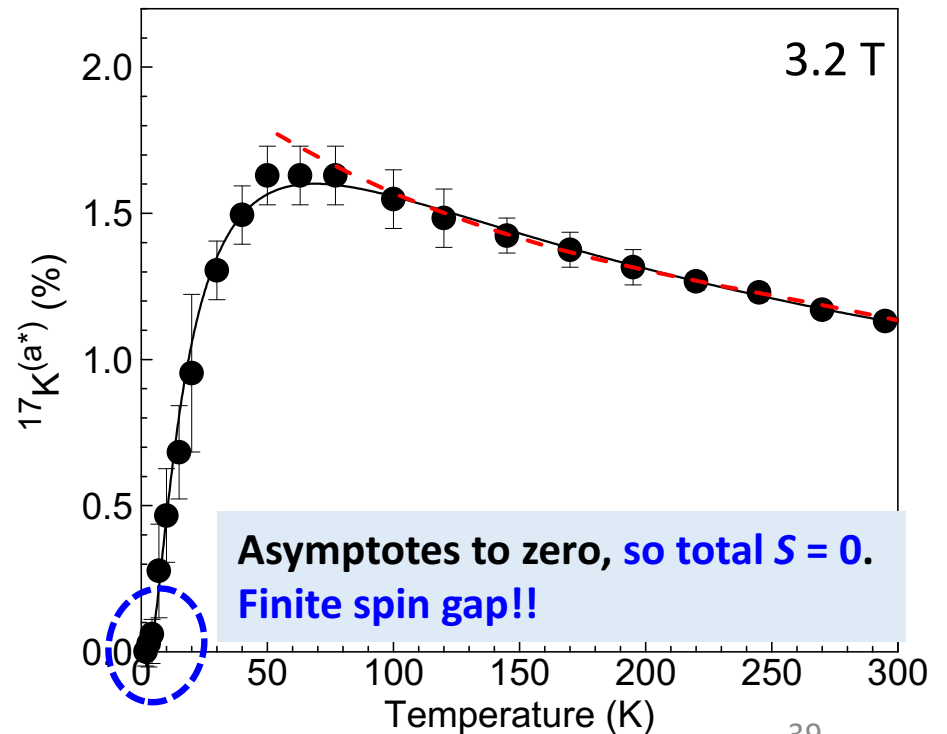
# Intrinsic susceptibility $\chi_{\text{kagome}}$ of the kagome plane as determined from the $^{17}\text{O}$ Knight shift at the main sites measured with $B = 3.2 \text{ T} \parallel a^*$



Main1 only (measured with long RF pulses)

The optimal RF pulse width for Main1 is factor 2 ~ 3 times broader (because we flip all 5 transitions at the same time).

We can measure Main1 peak **selectively**, and observed the same results for  $^{17}\text{K}$ .

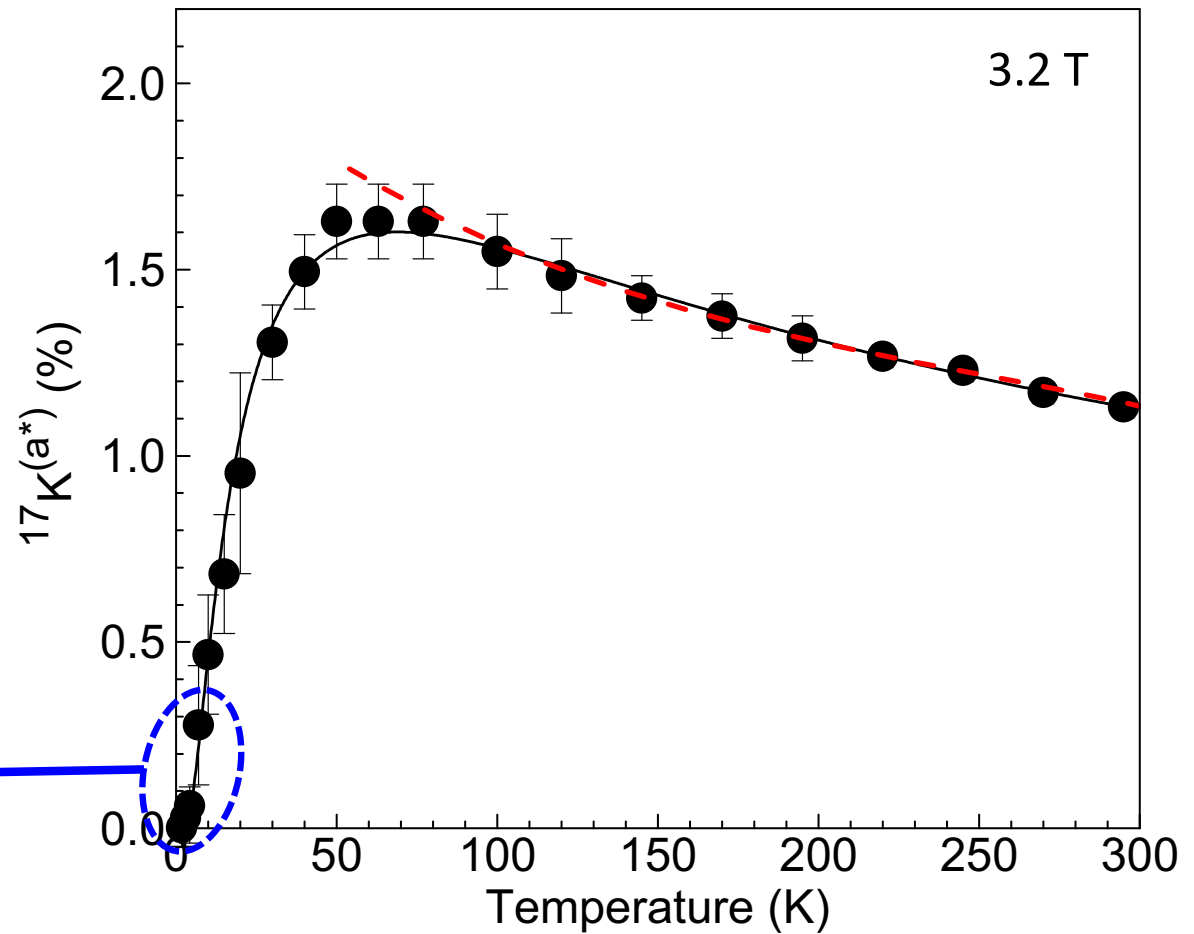
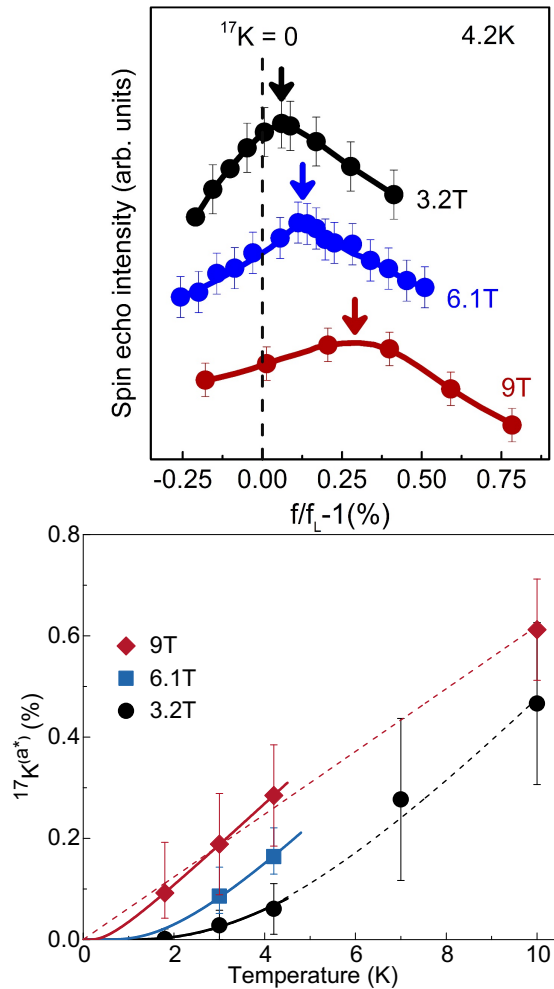


Asymptotes to zero, so total  $S = 0$ .  
Finite spin gap!!

→  
Larger frequency shift  
Larger  $^{17}\text{K}$  and  $\chi_{\text{kagome}}$

# Magnetic field dependence of the gap

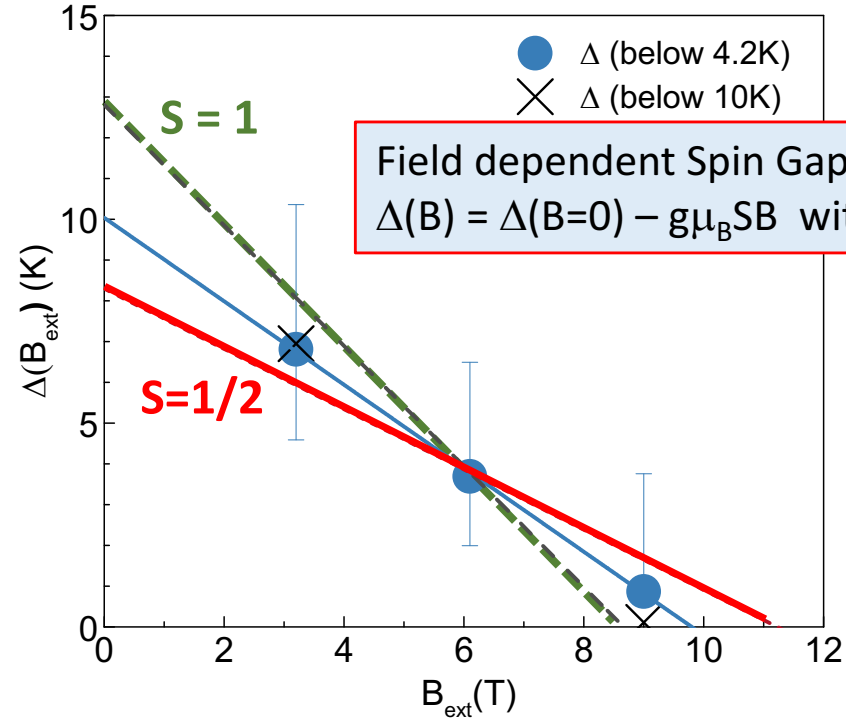
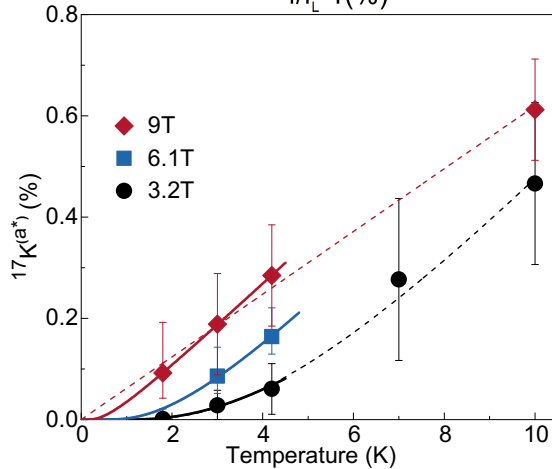
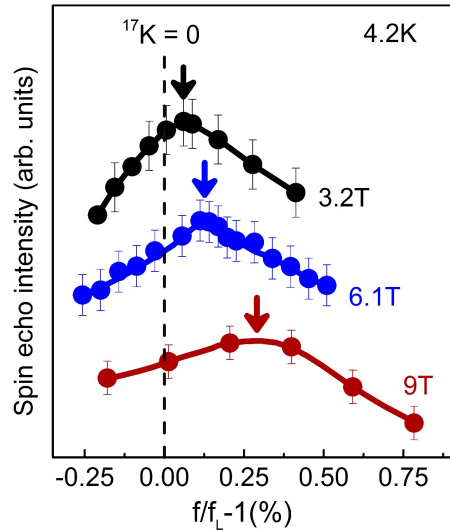
$^{17}\text{K}(\text{a}^*)$  depends on  $|B|$  below  $\sim 10\text{K}$



Solid (dashed) lines:  
 best fit to  $^{17}\text{K}(\text{a}^*) \sim T \cdot \exp(-\Delta/T)$  below 4.2 K (10 K).  
 Pre-factor T: to account for the expected decrease caused by SRO  
 (also arises in Dirac Fermion Model, P.A. Lee, private communications).

# Magnetic field dependence of the gap: $\Delta(B_{\text{ext}} \rightarrow 0) \sim 0.05J$

$^{17}\text{K}^{(a^*)}$  depends on  $|B|$  below  $\sim 10\text{K}$



Field dependent Spin Gap:  
 $\Delta(B) = \Delta(B=0) - g\mu_B SB$  with  **$S=1/2$  spinons**

$\Delta(0) \sim 10\text{ K}$ , hence  $\Delta(0) \sim 0.05\text{ J}$

Consistent with DMRG calculations, Yan *et al.*, *Science* (2011)

Note: we cannot entirely rule out  **$S = 1$**  excitations.

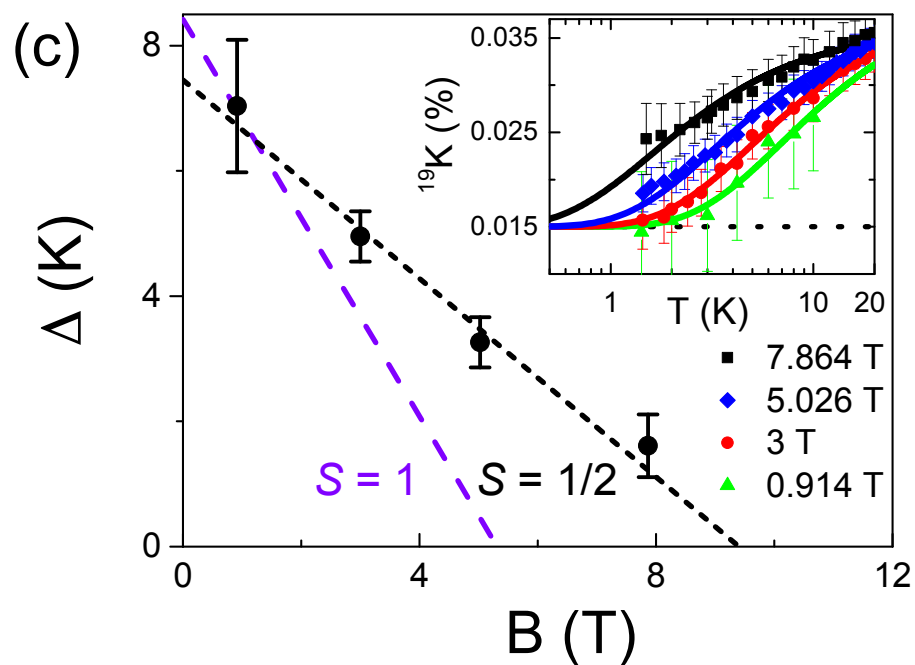
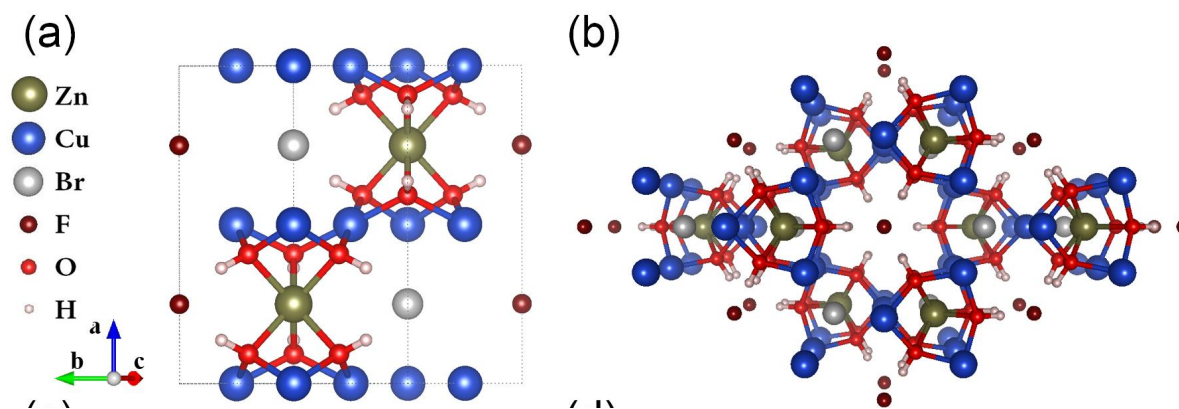
Solid (dashed) lines:

best fit to  $^{17}\text{K}^{(a^*)} \sim T * \exp(-\Delta/T)$  below 4.2 K (10 K).

Pre-factor T: to account for the expected decrease caused by SRO (also arises in Dirac Fermion Model, P.A. Lee, private communications).

# Spin $\frac{1}{2}$ excitations in Barlowite $\text{Cu}_3\text{Zn}(\text{OH})_6\text{FBr}$ from $^{19}\text{F}$ NMR (?)

Z. Feng, G.-q. Zheng et al.  
arXiv:1702.01658



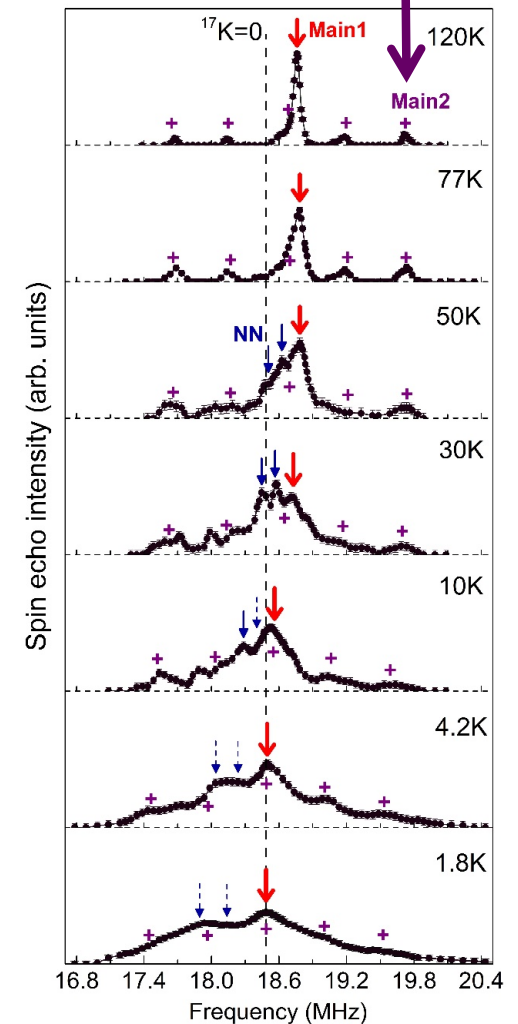
# Additional evidence for a finite gap $\Delta$ based on low-frequency spin dynamics

$^{17}\text{O}$  nuclear spin-lattice relaxation rate  $1/T_1$  at Main2 sites

We measured  $1/T_1$  in  $B = 3.2$  or  $9$  T using the isolated, clean, upper-most Main2 satellite peak for the  $I_z = 3/2$  to  $5/2$  transition to obtain reliable results.

$$\frac{M(t)}{M(\infty)} = 1 - [0.0714 \cdot e^{-15t/T_1} + 0.2857 \cdot e^{-10t/T_1} + 0.4 \cdot e^{-6t/T_1} + 0.2143 \cdot e^{-3t/T_1} + 0.0286 \cdot e^{-t/T_1} +]$$

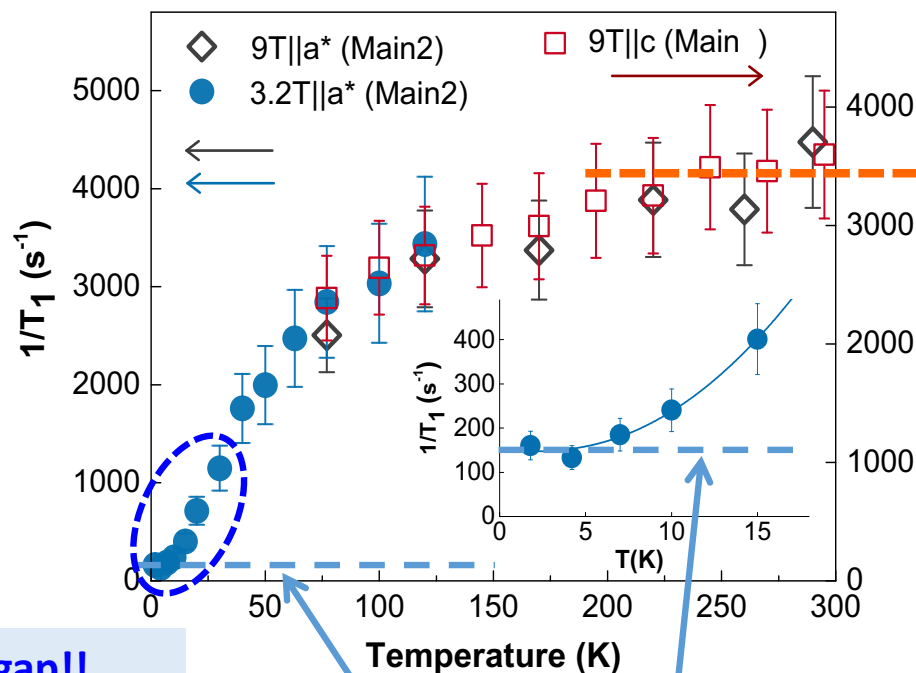
**Note:** this is the only way to measure  $1/T_1$  accurately at the  $^{17}\text{O}$  sites, even though the signal intensity is miserably small!



# Additional evidence for a finite gap $\Delta$ based on low-frequency spin dynamics

## $^{17}\text{O}$ nuclear spin-lattice relaxation rate $1/T_1$ at the Main site

$$\frac{1}{T_1} \propto T \cdot \sum_{\vec{q}} |A_{hf}(\vec{q})|^2 \frac{\chi''(\vec{q}, f_{NMR})}{f_{NMR}} \sim \sum_{\vec{q}} |A_{hf}(\vec{q})|^2 S(\vec{q}, f_{NMR})$$

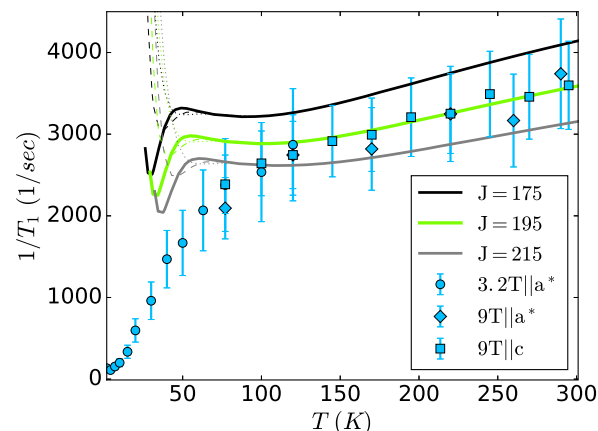


$$\left(\frac{1}{T_1}\right)_\infty \sim \frac{A_{hf}^2}{J} \sim 3,300 \text{ sec}^{-1}$$

Parameter-free theoretical estimation in the high temperature limit ( $T \gg J$ ) based on Moriya's Gaussian approximation applied to kagome Heisenberg model ( $J = 180 \text{ K}$ )

Spin gap!!  
 $\Delta \sim 7 \text{ K}$  in 3.2T

Defect contribution  
(in-gap excitations)



N.Sherman, T.I., R.R.P. Singh  
PRB 94 (2016) 140415(R).

# A comparable gap $\Delta$ deduced from inelastic neutron scattering

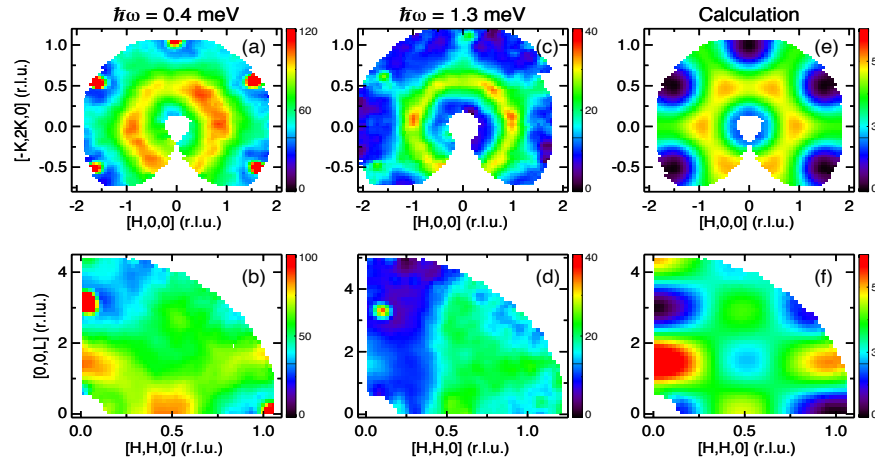
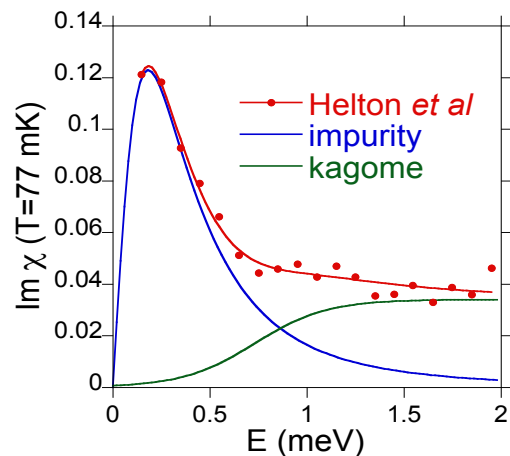


FIG. 12 (Color online) Momentum structure of the INS data at 0.4 meV and 1.3 meV for single crystal herbertsmithite at 2 K in the (HK0) scattering plane (top row) and (HHL) scattering plane (bottom row) (Han *et al.*, 2015). The plots in the right column are the calculated structure factor for near neighbor AF correlations between copper defects on the zinc sites, taking into account the copper form factor. These correspond to correlations between the brown and the gray sites of Fig. 1, which sit in successive triangular planes.

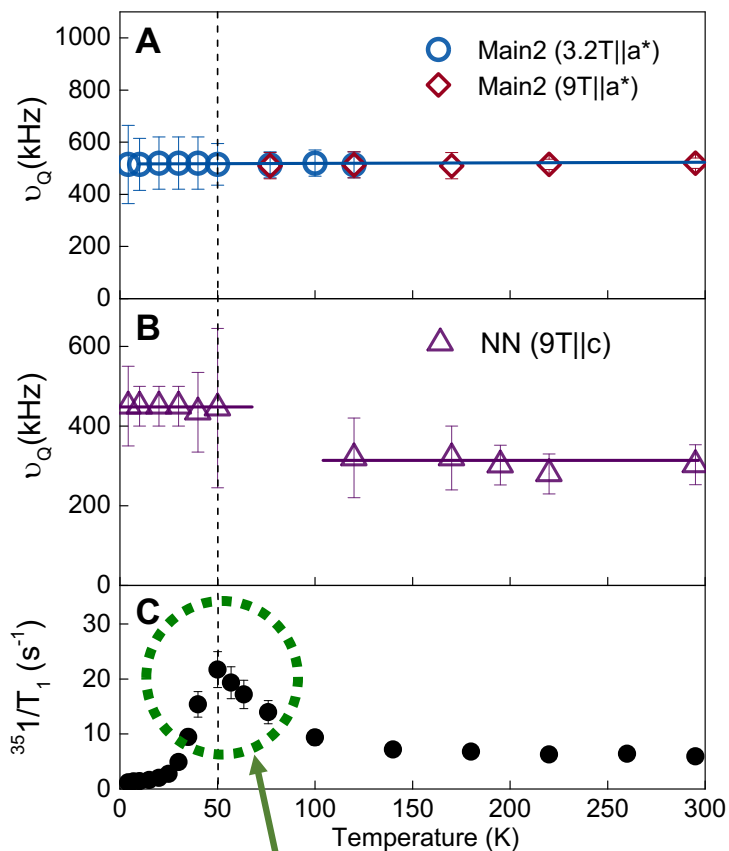


Magnitude of gap comparable to NMR results

T.-H. Han, M. Norman, Y.S. Lee *et al.*  
PRB (2016). Arxiv:1604.03048

# Additional complications caused by defects

Supplementary Materials, Science (2015) Fu, T.I. et al



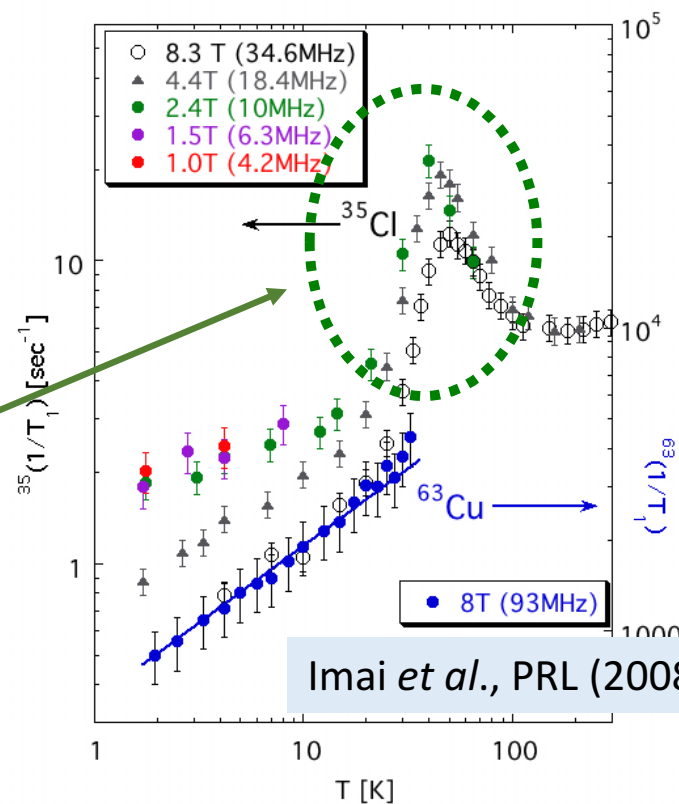
$\nu_Q$  stays constant for the Main $^{17}\text{O}$  sites

*Average structure of the kagome plain remains unchanged*

$\nu_Q$  changes for the NN  $^{17}\text{O}$  sites

*Local structure deforms near the defects.*

Bump of  $1/T_1$  at  $^{35}\text{Cl}$  sites; depends on frequency.  
*Something is slowly freezing below 50K.*



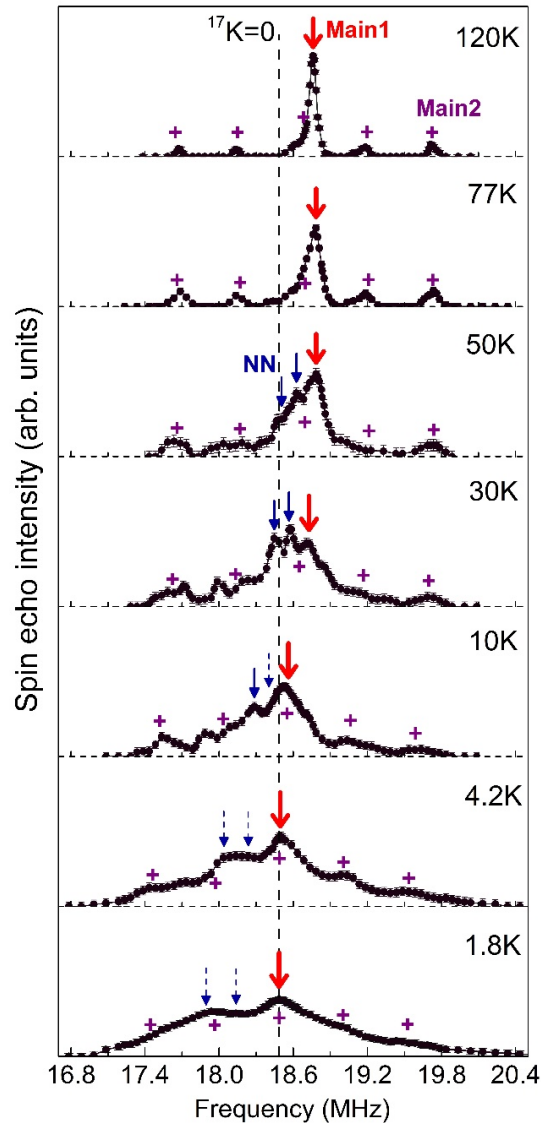
Imai et al., PRL (2008)

## Key Conclusions

- $\text{Cu}^{2+}$  defect spins occupy the Zn sites with  $\sim 15\%$  probability;  $(\text{Zn}_{0.85}\text{Cu}_{0.15})\text{Cu}_3(\text{OH})_6\text{Cl}_2$ .
- Defect spins exhibits Curie-Weiss behavior:  $\chi_{\text{defect}} \sim C/(T + \theta)$  with  $\theta \sim +1$  K.
- No evidence for Zn anti-site defects at the kagome Cu sites in anomalous X-ray, powder Rietveld refinement,  $^2\text{D}$  single-crystal NMR, nor  $^{17}\text{O}$  single crystal NMR.
- kagome spin susceptibility  $\chi_{\text{kagome}} \rightarrow 0$  at  $T = 0$  with a small, field-dependent gap;  $\Delta \sim 0.05\text{J}$ .
- Lattice deformation freezes in the immediate vicinity of defects below  $\sim 50$  K;  
(Open question) effects on the overall magnetism of the kagome planes?

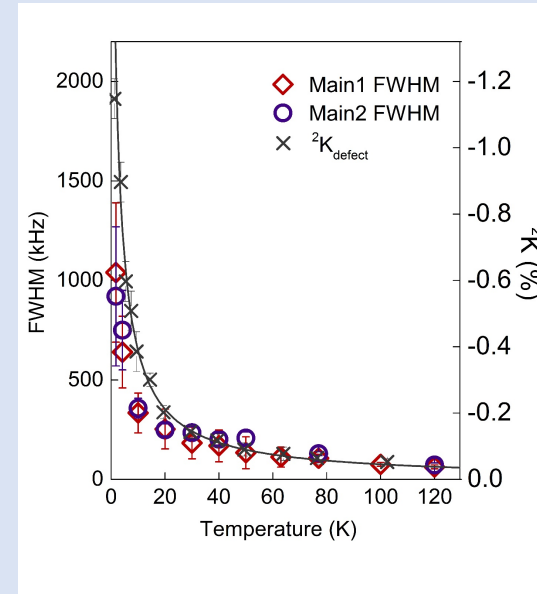
Thank you for your attention!

# Intrinsic susceptibility $\chi_{\text{kagome}}$ of the kagome plane as determined from the $^{17}\text{O}$ Knight shift at the main sites measured with $B = 3.2 \text{ T} \parallel a^*$



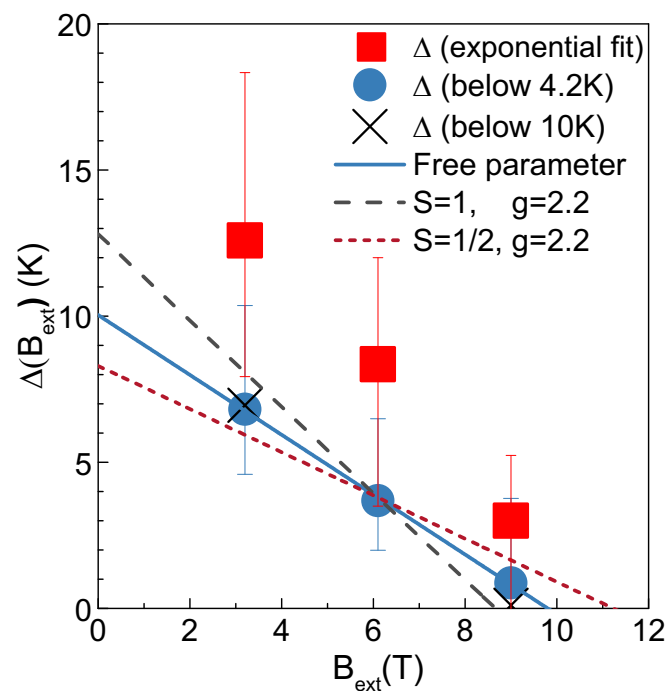
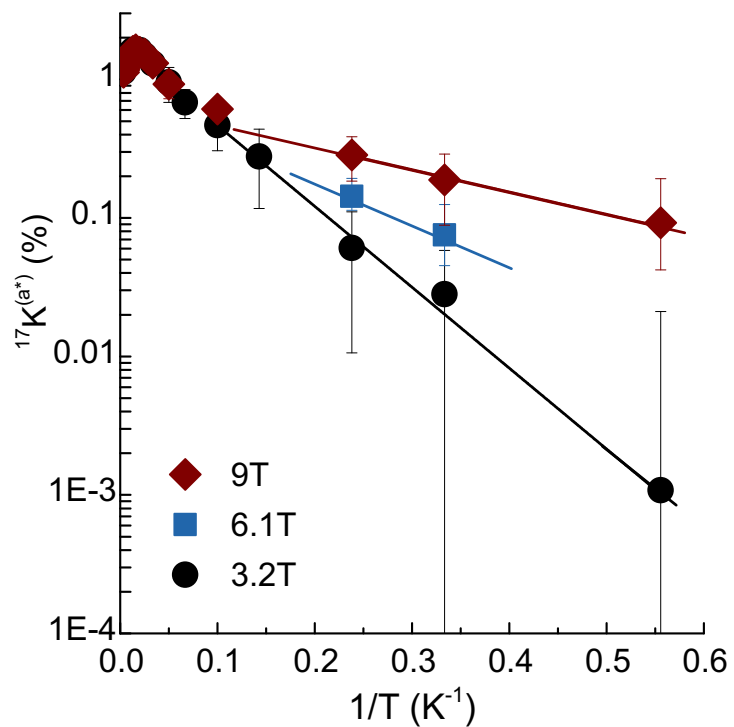
Larger frequency shift  
 Larger  $^{17}K$   
 Larger  $\chi_{\text{kagome}}$

- All NMR lines broaden in proportion to  $\chi_{\text{defect}}$ .



- But we can trace the Main1 peak down to 1.8 K ( $\sim 0.01\text{J}$ ), because it is singularly larger than all other peaks.
- Main1 peak frequency reaches a maximum at  $\sim 60\text{K}$ , then **shifts back to the zero Knight shift position at low temperatures.**
- We cannot resolve the central peak of Main2, but its uppermost satellite peak displays qualitatively the same trend.

# Magnetic field dependence of the gap --- alternate fits with a simple exponential function



Semi-quantitatively the same results for  $\Delta$